Ecological Applications, 24(5), 2014, pp. 1037–1056

Climate, fire size, and biophysical setting control fire severity and spatial pattern in the northern Cascade Range, USA

C. Alina Cansler[1,3] and Donald McKenzie[2]

[1]*School of Environmental and Forest Sciences, University of Washington, Seattle, Washington 98195-2100 USA*
[2]*Pacific Wildland Fire Sciences Lab, USDA Forest Service, Seattle, Washington 98103 USA*

Abstract. Warmer and drier climate over the past few decades has brought larger fire sizes and increased annual area burned in forested ecosystems of western North America, and continued increases in annual area burned are expected due to climate change. As warming continues, fires may also increase in severity and produce larger contiguous patches of severely burned areas. We used remotely sensed burn-severity data from 125 fires in the northern Cascade Range of Washington, USA, to explore relationships between fire size, severity, and the spatial pattern of severity. We examined relationships between climate and the annual area burned and the size of wildfires over a 25-year period. We tested the hypothesis that increased fire size is commensurate with increased burn severity and increased spatial aggregation of severely burned areas. We also asked how local ecological controls might modulate these relationships by comparing results over the whole study area (the northern Cascade Range) to those from four ecological subsections within it. We found significant positive relationships between climate and fire size, and between fire size and the proportion of high severity and spatial-pattern metrics that quantify the spatial aggregation of high-severity areas within fires, but the strength and significance of these relationships varied among the four subsections. In areas with more contiguous subalpine forests and less complex topography, the proportion and spatial aggregation of severely burned areas were more strongly correlated with fire size. If fire sizes increase in a warming climate, changes in the extent, severity, and spatial pattern of fire regimes are likely to be more pronounced in higher-severity fire regimes with less complex topography and more continuous fuels.

Key words: bottom-up controls; burn severities; climate change; fire regimes; FRAGSTATS; North Cascades, Washington, USA; patch dynamics; relative differenced normalized burn ratio; RdNBR; remote sensing; top-down controls; topography.

Introduction

In western North America, the annual area burned by wildfires has substantially increased since the mid-1980s. Two main factors are believed to be driving the increase in area burned: (1) increased vertical and horizontal continuity of fuels due to previous fire suppression and other land-use practices such as logging and grazing (Hessburg et al. 2005), and (2) warmer and drier climate (Littell et al. 2010). Contemporary and historical records demonstrate that larger fires and greater area burned are positively correlated with warm and dry climate across a wide range of forest ecosystems (Heyerdahl et al. 2008*a*, *b*, Littell et al. 2009, Lutz et al. 2009, Miller et al. 2012*a*, Abatzoglou and Kolden 2013). Because climate change is expected to increase the length of summer drought, and the connectedness and flammability of fuels across the landscape, a significant increase in area burned is expected under climate change (Flannigan et al. 2009, 2013, Littell et al. 2010, Wotton et al. 2010).

Manuscript received 7 June 2013; revised 19 September 2013; accepted 4 November 2013. Corresponding Editor: C. H. Sieg.
[3] E-mail: acansler@uw.edu

These increases in area burned could have both desirable and adverse ecological impacts. In most ecosystems in western North America, plant and animal species evolved with fire and are adapted to it (Agee 1993, Sugihara et al. 2006). If fires burn in a way that restores pattern, structure, and function to that of pre-Euroamerican settlement, the increased area burned might help to maintain current ecosystem function and species diversity, and to increase ecosystems' resilience to a changing climate and subsequent disturbances. On the other hand, if increases in area burned bring changes in other fire-regime attributes, such as frequency, extent, spatial pattern, and severity or fires, the ecological effects of the fire will have changed and the ecosystem may be altered (Pickett and White 1985, Agee 1993, Sugihara et al. 2006).

Our understanding of large-fire growth and extreme fire behavior supports a connection between increased fire size and increased burn severity and spatial aggregation of severely burned areas. Here we define burn severity as the ecological effect of the fire on soils and plants, which includes the direct consumption of organic materials by the fire and delayed ecosystem responses, such as tree mortality, vegetation resprouting, and colonization of new propagules (Cansler and McKenzie 2012). Because large fires tend to occur during periods of extreme fire behavior, we would expect increases in fire size to be correlated with increased severity and large, homogenous high-severity patches. For example, based on observations of severity and spatial pattern of the 1988 fires in Yellowstone National Park and simulation modeling, Turner and Romme (1994) hypothesized that extreme fire weather overrides the influence of local controls such as topography and fuels, causing extreme fire behavior and rapid fire growth.

The probability of weather and climate overriding local controls depends on both the strength of local controls and of the characteristic intensity of the fire regime (Agee 1997, Haire and McGarigal 2009, Thompson and Spies 2009). In high-severity fire regimes with weak local controls, such as *Pinus contorta* var. *latifolia* (lodgepole pine)-dominated forests of the Greater Yellowstone Ecosystem or boreal forests with relatively gentle topography, warm, dry climate and extreme weather produce synchronous fire behavior across the landscape (Turner and Romme 1994, Bessie and Johnson 1995). In forests with complex terrain, however, such as the Cascade Range, barriers to fire spread are present even under extreme climate and weather (Prichard and Kennedy 2012). In low-severity fire regimes, such as dry *Pinus ponderosa* (ponderosa pine) forests in which frequent fire or other processes have maintained fine-scale heterogeneity in fuels, fire-resistant traits of the dominant vegetation make synchronous high-severity fire less likely, even under extreme climate.

The goal of this study is to connect changes in climatic drivers of area burned and fire size with changes in the ecological effects of the fire in the northern Cascade Range of Washington State, USA. We focus on burn severity and burn-severity pattern, two fire-regime attributes that influence other ecosystem processes. Severity affects the composition and timing of postfire succession (Turner et al. 1997, 1999, Lentile et al. 2007); geomorphic process, such as the movement of water and sediment across the landscape (Swanson 1981); biogeochemical and belowground process, such as soil nutrient composition, physical properties, and microbial populations (Neary et al. 1999, Smithwick 2011); and wildlife habitat suitability (Roberts et al. 2008, Wightman et al. 2010, Dudley et al. 2012, Buchalski et al. 2013). The burn-severity pattern also influences postfire succession, and in some systems the severity and spatial pattern of previous disturbances can affect subsequent disturbance (Peterson 2002, McKenzie et al. 2011, Haire et al. 2013). In large high-severity patches, seed sources from wind- and animal-dispersed species may be limited, influencing the timing and composition of subsequent vegetation establishment and nutrient availability (Turner et al. 1994, Donato et al. 2009). In low-severity fire regimes, heterogeneous patterns of burn severity facilitate tree regeneration, allowing trees to survive long enough to express fire-resistant traits such as thick bark (Agee 1993). Knowledge of how severity and its spatial patterns may change with increased fire extent suggests how other ecosystem processes may shift under climate change and what types of climate adaptation could be used to maintain ecosystem resilience into the future.

Objectives

There were three objectives to this study: (1) to examine the relationships between local climate and fire extent, (2) to test if area burned is correlated with severity and the spatial pattern of high-severity areas, and (3) to ascertain how local environmental and ecological variability meditate the relationship between fire size and burn severity or burn-severity pattern. To achieve the last, we conducted our analyses at two scales: across our whole study area, the northern Cascade Range of Washington, USA, and separately for four ecological subsections within the larger study area (Fig. 1). These subsections have different climate, topography, and vegetation, which we expected would produce different fire regimes. At each spatial extent, we tested the hypotheses that fire size is correlated with burn severity, and fire size is correlated with increased spatial aggregation of high severity. Metrics for the latter include attributes of patch-size distributions at varying scales.

Methods

Study area

The study area encompasses 1 445 500 ha of federally managed land in the northern Cascade Range, from the western boundaries of North Cascades National Park and Glacier Peak Wilderness to the eastern boundary of the Okanogan-Wenatchee National Forest. The U.S.–Canadian border is the northern boundary and WA State Highway 2 is the southern boundary. Fifty percent (729 200 ha) of the study area is protected as wilderness. Vegetation within the study area changes gradually from moist forests on the west side of the crest of the Cascade Range to dry forests on the east side, reflecting gradients in climate, soil types, and elevation (Franklin and Dyrness 1988). In most of the study area, fire regimes are of high or mixed severity.

Ecological variation within the study area: ecological subsections

We used ecological subsections as the basis for delineating ecologically similar regions within our study area. Ecological subsections represent the smallest mapping unit identified under the USDA Forest Service's National Hierarchical Framework; larger ecosections have been in use for over 30 years and refined through subsequent peer review (Cleland et al. 1997, ECOMAP 2007). Ecological subsections were demarcated based on climatic gradients, physiographic and geologic substrate, patterns in potential vegetation, soil groups, and hydrography. After visually evaluating

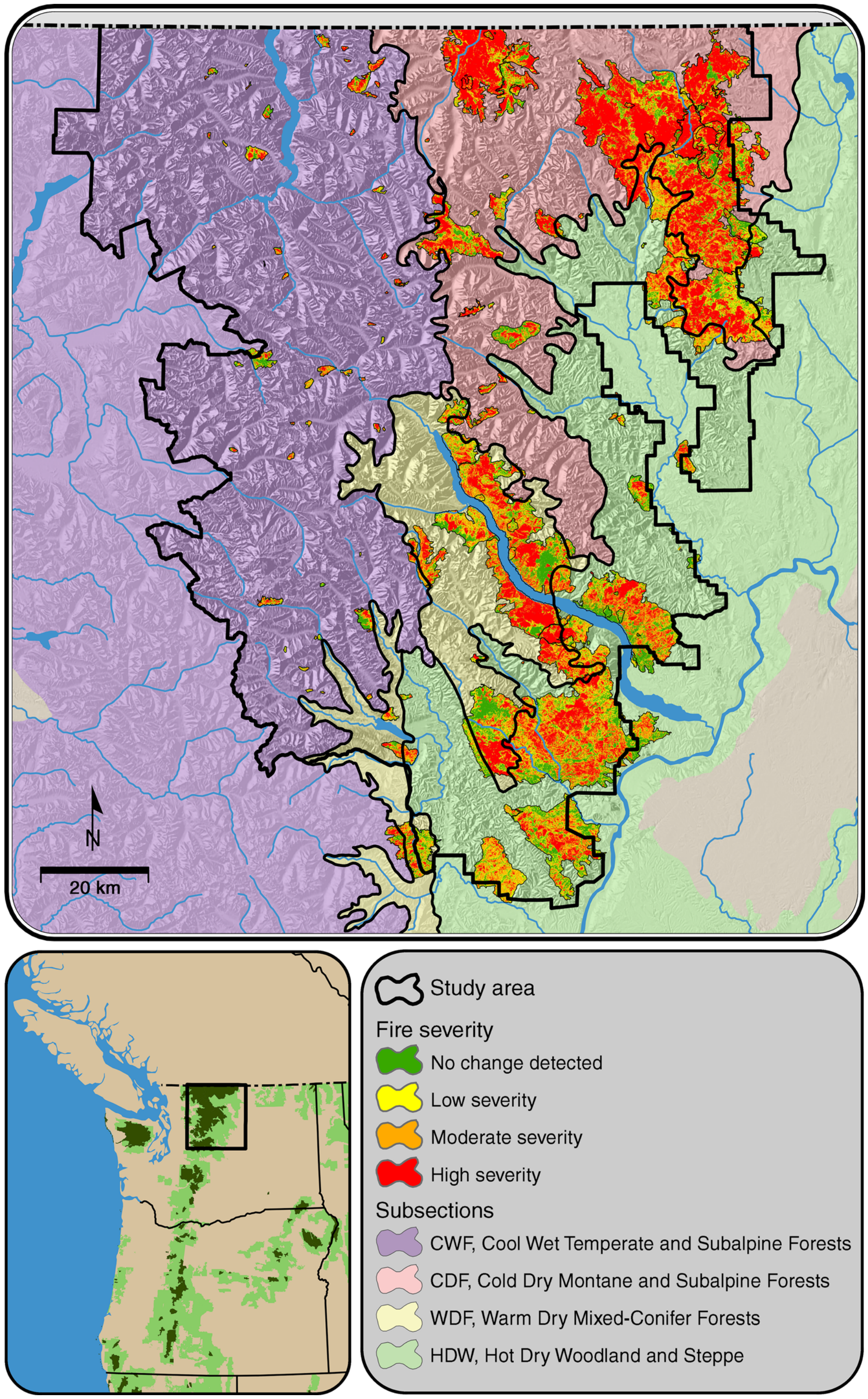

FIG. 1. Map of the burn severity of all 125 fires included in the study, overlaying the four ecological subsections used in this study. The insert reference map shows the location of the study area in the northern Cascades of northern Washington State, USA, adjacent to the U.S.–Canada border, with federal forest lands shown in light green, and lands in protected status (national parks, federally designated wilderness areas) shown in dark green.

TABLE 1. Climate, topographical variability, and vegetation types within each USDA Forest Service ecological subsection in the Northern Cascades, Washington, USA.

Variable	CWF	CDF	WDF	HDW
Climate†				
Annual maximum temperature (°C)	9 (0 to 15)	7 (3 to 14)	10 (3 to 17)	12 (7 to 17)
Annual minimum temperature (°C)	0 (−9 to 5)	−2 (−6 to 1)	0 (−6 to 4)	1 (−3 to 5)
July maximum temperature (°C)	20 (11 to 29)	20 (15 to 28)	22 (14 to 32)	26 (18 to 32)
January minimum temperature (°C)	−6 (−14 to 0)	−8 (−11 to −6)	−7 (−12 to −3)	−7 (−10 to −4)
Annual precipitation (cm)	208 (83 to 458)	107 (43 to 199)	111 (30 to 268)	64 (24 to 137)
Topographical variability				
Mean elevation (m)	1450	1785	1386	1039
Elevation range (m)	106 to 3213	624 to 2714	335 to 2875	256 to 2189
Vegetation or cover type‡ (ha and %)				
T. heterophylla/P. menziesii/T. plicata/P. sitchensis	206 617 (35%)	5343 (2%)	12 368 (7%)	3658 (1%)
Alpine/subalpine meadow or shrubland	78 661 (13%)	54 199 (15%)	17 637 (10%)	1392 (0%)
T. mertensiana	112 311 (19%)	3384 (1%)	3861 (2%)	35 (0%)
P. albicaulis	24 182 (4%)	62 219 (18%)	16 485 (10%)	583 (0%)
P. engelmannii/A. lasiocarpa/P. contorta	25 482 (4%)	97 146 (28%)	17 009 (10%)	4293 (1%)
P. menziesii/A. grandis	11 867 (%)	2500 (1%)	18 477 (11%)	23 050 (7%)
P. ponderosa/P. menziesii	10 874 (2%)	84 282 (24%)	49 193 (29%)	179 799 (55%)
Shrubland and grassland	52 920 (9%)	31 349 (9%)	18 665 (11%)	93 781 (29%)
Hardwood and riparian	12 875 (2%)	4668 (1%)	4940 (3%)	10 389 (3%)
Nonflammable/unlikely to burn (water, ice, barren, or sparse)	60 392 (10%)	7062 (2%)	11 395 (7%)	9916 (3%)
Total area (ha)	596 444	352 173	170 030	326 897

Note: Ecological subsection abbreviations are CWF, Cool Wet Temperate and Subalpine Forests; CDF, Cold Dry Montane and Subalpine Forests; WDF, Warm Dry Mixed-Conifer Forests; HDW, Hot Dry Woodland and Steppe.

† All climate variables are based on 1981–2010 averages from 4-km resolution PRISM gridded climate data (available at http://prism.oregonstate.edu; Daly et al. 2002*a*). Ranges reflect spatial variation in gridded climate data within the subsection; 425, 255, 115, and 229 grid cells were used in the CWF, CDF, WDF, and HDF, respectively.

‡ Classes are based on LANDFIRE existing vegetation layer (Rollins and Frame 2006; data available online at www.landfire.gov). Areas are given in hectares with percent cover within each subsection shown in parentheses. Species are *Abies grandis* (grand fir), *Abies lasiocarpa* (subalpine fir), *Picea engelmannii* (Engelmann spruce), *Picea sitchensis* (Sitka spruce), *Pinus albicaulis* (whitebark pine), *Pinus contorta* var. *latifolia* (lodgepole pine), *Pinus ponderosa* (ponderosa pine), *Pseudotsuga menziesii* var. *menziesii* (Douglas-fir), *Thuja plicata* (western redcedar), *Tsuga heterophylla* (western hemlock), *Tsuga mertensiana* (mountain hemlock).

geospatial layers of vegetation, fuels, and climate for similarities in relation to subsection boundaries, we developed four subsections that capture differences in vegetation, climate, and physiography within our study area (Fig. 1; original ecological subsections used as a basis for those in this study are in Appendix A: Fig. A1).

The Cool Wet Temperate and Subalpine Forests (CWF) have moderate summer temperatures and the highest annual precipitation and the most complex topography of all the subsections (Table 1; Appendix A: Figs. A2–A5). Low- and mid-elevations forests, dominated by *Tsuga heterophylla* (western hemlock), *Pseudotsuga menziesii* var. *menziesii* (Douglas-fir), and *Abies amabilis* (Pacific silver fir), have a low-frequency high-severity fire regime (Agee 1993). Montane forests near Ross Lake, near the center of the subsection, may burn more frequently (75–140 years) with mixed severity, and have highly variable fire-return intervals that respond to synoptic changes in climate over long time scales (Agee et al. 1990, Prichard et al. 2009). This subsection contains North Cascades National Park Complex, within which wildland fires have been allowed to burn for resource benefit since 1991. Nonflammable areas, such as lakes, glaciers, permanent snowfields, and barren rocky areas, and other areas where fire may be virtually absent due to continuously high fuel moisture, are prevalent in the CWF (Agee et al. 1985).

The Cold Dry Montane and Subalpine Forests (CDF) include higher, cooler, and drier areas in the northeast part of the study area. This subsection also has less complex topography and large areas of continuous subalpine forests. Mid-elevation forests in the CDF feature *Abies lasiocarpa* (subalpine fir) and *Picea engelmannii* (Engelmann spruce), although *A. amabilis*, *Larix occidentalis* (western larch), and *Pinus contorta* (lodgepole pine) are also common (Fahnestock 1976), the latter two in the eastern portion. The *A. lasiocarpa*/*P. engelmannii* forests extend into subalpine areas. *Pinus albicaulis* (whitebark pine) forests with a significant component of *Larix lyallii* (subalpine larch) are common at timberline (Table 1). Fire regimes in the CDF are more similar to those in the northern Rocky Mountains than to subalpine areas in the Cascade Range, reflecting drier interior climate and the mixture of interior tree species (Fahnestock 1976, Franklin and Dyrness 1988).

The Warm Dry Mixed-Conifer Forests (WDF), located in the center of the study area east of the crest of the Cascades, include mid-elevation mixed-conifer forests (*Pinus ponderosa*, *P. menziesii* var. *glauca*, and *Abies grandis* [grand fir]), subalpine forests, and alpine areas. This subsection has a climate similar to the CDF, but with slightly drier and warmer summers, and most of the area is lower in elevation, with more complex topography. Much of this subsection is in the drainage of Lake Chelan, a glacially formed lake, 1 mile wide by 55 miles long. Historically it had a predominantly mixed-severity fire regime (Hessburg et al. 2007).

The Hot Dry Woodland and Steppe (HDW) includes lower-elevation areas on the east side of the study area with low winter snowpack and high summer temperatures, with dry (*P. menziesii*/*P. ponderosa*) mixed-conifer forest. A low-severity fire regime was characteristic of the open grasslands and *P. ponderosa* parkland present at lower elevations (Agee 1993).

Burn-severity atlas development

Geospatial fire-occurrence data from federal land management agencies (National Park Service and U.S. Forest Service) were used to identify all fires > 10 ha that occurred in the study area from 1984 to 2008; 125 fires met the criterion (Appendix A: Table A4). Landsat satellite imagery (30-m resolution) and the Relative differenced Normalized Burn Ratio (RdNBR), a spectral burn-severity index based on the near- and mid-infrared portions of the electromagnetic spectrum (Miller and Thode 2007), were used to map burn severity (formula in Appendix A: Table A3). Higher values of RdNBR indicate higher burn severity. RdNBR and similar indices have been validated extensively with field data in temperate conifer forests (Miller et al. 2009*a*, Soverel et al. 2010, Cansler and McKenzie 2012). To compute the index, we used cloud-free Landsat image pairs with matching phenology, usually from the year before and the year after the fire, unless quality concerns dictated a longer interval. Some clouds were present in seven fire images, but made up $<1\%$ of the area burned in the study area or any subsection and were masked out of all analyses of severity and severity pattern. The image pairs were processed according to existing MTBS (Monitoring Trends in Burn Severity) protocols by the USGS National Center for Earth Resources Observation and Science (EROS) (Eidenshink et al. 2007).

Fire and climate

Climate variables were analyzed at the scale of the study area and for each ecological subsection. We acquired 4-km resolution (1600-ha) monthly maximum mean temperature, mean dew point temperature, and precipitation data from PRISM (Daly et al. 2002; PRISM data *available online*).[4] The mean raster value for each observation of each climate variable was calculated within each analysis area. Gridded climate data can be influenced by the changes in the quality and total number of climate stations that are used as a basis to interpolate climate. Because additional weather monitoring stations were established during the study period, we also developed regressions at the scale of the study area using monthly climate data from two weather monitoring stations centrally located within the study area that had consistent high-quality records. These data include mean temperature (May–September) and total monthly precipitation data from the Stehekin COOP station (48°21′ N, 120°43′ W, 387 m above sea level) through the United States Historical Climatology Network (USHCN; data *available online*).[5] We acquired peak spring snow water equivalent (SWE) data (1 May; based on the median date of peak snow accumulation over the period of record) from an automated snow telemetry station (SNOTEL), the Lyman Lake SNOTEL station, 48°12′ N, 120°55′ W, 1823 m a.s.l. (data *available online*).[6] PRISM data and climate station temperature and precipitation data spanned the entire study period (1984–2008; $n = 25$); analysis of SWE data is limited to 1985–2008 ($n = 24$), due to missing observations in 1984. Both the PRISM and climate station precipitation data were summarized by season.

In total, we used 13 climate variables from the PRISM data set and eight climate variables from the climate stations. Seven variables are related to the intensity of drought during the summer (summer precipitation, July, August, and September temperature, and July, August, and September dew point [PRISM only]), and five are related to moisture availability early in the fire season (spring SWE [climate station only], winter precipitation [PRISM only], spring precipitation, May, June temperature, and May, June dew point [PRISM only]). The majority of fires > 10 ha started in July and August ($\sim 65\%$), and thus the summer precipitation July and August temperature probably reflected the climate and weather during the peak of the fire season in the study area.

We used linear regression to test whether climate variables were significant predictors of annual area burned and annual mean fire size. All climate data were normalized and all area measurements were $\log_{10}$-transformed for analysis, to compensate for the right-skewed area data. Regressions were built as conditional models, and only used data from years in which fires $>$ 10 ha occurred. Predictor variables or two-way interactions that were independently significant ($\alpha = 0.1$) were included. We then used backward elimination ($\alpha = 0.05$) to select the minimum adequate model (the model that explained the most variance with the fewest variables). Likelihood ratio tests were used to choose among linear regression models. In cases where multiple models were similarly plausible, we present more than one model.

[4] http://www.prism.oregonstate.edu

[5] http://cdiac.ornl.gov/epubs/ndp/ushcn/access.html

[6] http://www.wcc.nrcs.usda.gov/nwcc/site?sitenum=606&state=WA

Fire size and burn severity

We measured the severity of each fire using both the continuous and categorized RdNBR values. The continuous RdNBR images were converted into categorical burn-severity images, with four classes: no change detected, and low, moderate, and high severity (Miller and Thode 2007, Cansler and McKenzie 2012); see Appendix A: Table A1. Burn-severity class thresholds were developed based on regressions with field-based burn-severity data from 639 field plots located across four fires (Cansler and McKenzie 2012). Overall classification accuracy was 62% and classification was 40% better than a random classification, within the range found by similar studies in California and Canada (Miller and Thode 2007, Soverel et al. 2010). Classification accuracies of the high-severity class, emphasized in this study, were better or equal to the overall classification. Derived classification thresholds were used to create four-class categorical burn-severity images for all fires.

To measure the severity using continuous (unclassified) RdNBR values, we approximated a numerical integration of the area under the cumulative severity distribution and calculated the "severity metric," SM (Lutz et al. 2011), for each fire as one minus the normalized area under the curve (see Appendix A: Table A3 for equation). Fires that have a greater proportion of their pixels in high RdNBR values will have less area under the cumulative distribution curve and thus a higher SM, indicating that they burned with higher severity. To compare fires, RdNBR values were limited to those between −450 and 1425 (encompassing 99% of the pixel values over all fires). For fires with unimodal RdNBR distributions, such as those in this study, the SM is highly correlated with the mean. We used the SM instead of the mean because doing so allows for comparisons of burn severity between ecosystems with very different burn-severity distributions, such as the unimodal distributions found in many temperate forests, and the bimodal distributions sometimes observed in boreal forest. Using classified and continuous severity data allowed the satellite index to be related to observed fire effects on the ground while also revealing any biases that are artifacts of categorizing the original continuous data into four classes.

We used simple linear regression to test whether fire size is a significant predictor ($\alpha = 0.05$) of the SM and proportional area in each of the four fire-severity classes. For the latter, we treated each severity class separately, although theoretically for data categorized into n categories, only $n - 1$ of the tests are truly independent, as the last category is based on the combined proportions of the other $n - 1$ categories. Fire sizes were $\log_{10}$-transformed to account for the right skew of the data. The SM (range 0, 1) and the proportions were arcsine square-root transformed for analysis (Kutner et al. 2005). For all models in which the response variable was transformed (for this analysis and for the analysis of spatial pattern metrics to be described), we evaluated model fit based on normal probability plots, residual plots, and partial residual plots, and identified and evaluated appropriate transformations using the Box-Cox method (Kutner et al. 2005). Regressions were developed at the scale of study area and of each ecological subsection. In cases where a fire burned in more than one subsection, the fire was assigned to the subsection in which it burned the most area.

Fire size and burn-severity pattern

We restricted our analysis of within-fire burn-severity pattern to only the high-severity class. As discussed previously, the high-severity class is of concern in relation to climate-driven shifts in fire regimes, and can be classified with the greatest accuracy (Cansler and McKenzie 2012). We chose seven spatial-pattern metrics to quantify four aspects of spatial pattern: patch size, size inequality of patches, patch interior, and spatial aggregation at the grain of the pixel (30 m) (equations in Appendix A: Table A3). Most spatial pattern metrics were calculated with FRAGSTATS (McGarigal et al. 2002).

Patch size (two metrics).—We used two metrics of patch size: mean patch size and area-weighted mean patch size. The former gives equal weight to each patch, regardless of its size; the patches themselves are the population that the mean is quantifying. The latter weights each patch by its size, reflecting the patch size in which a randomly chosen pixel would most likely be found. In landscapes with a strongly right-skewed frequency distribution of patch sizes, such as the burn-severity patches in this study, there will be large differences between these two measures of patch size.

Size inequality (one metric).—We quantified the extent to which larger patches dominated the landscape with the Gini coefficient, which provides a relative measure of the size inequality of the patch distribution. Unlike mean patch size, the Gini coefficient is calculated relative to the minimum and maximum patch sizes observed, and therefore it is a robust method for comparing fires of different sizes, which intrinsically have different maximum patch sizes.

Patch interior (two metrics).—Core area is the area within patches greater than a specified distance from the edge of the patch. More core area implies large patches that are simple in shape, whereas less core area indicates small patches, patches with convoluted edges, or patches with interior areas of different severity. Regressions with fire size were based on the proportion of the core area that was more than 90 m from the edge of a patch. We have higher confidence that at a two-pixel depth within a patch, the patch actually did burn with high severity. Because the distance used to define core area could potentially influence regression results, we also conducted a post hoc sensitivity analysis of the effect of the distance used to define core area. We tested regressions predicting core area based on fire size from 30 m to 300 m (in 30-m intervals).

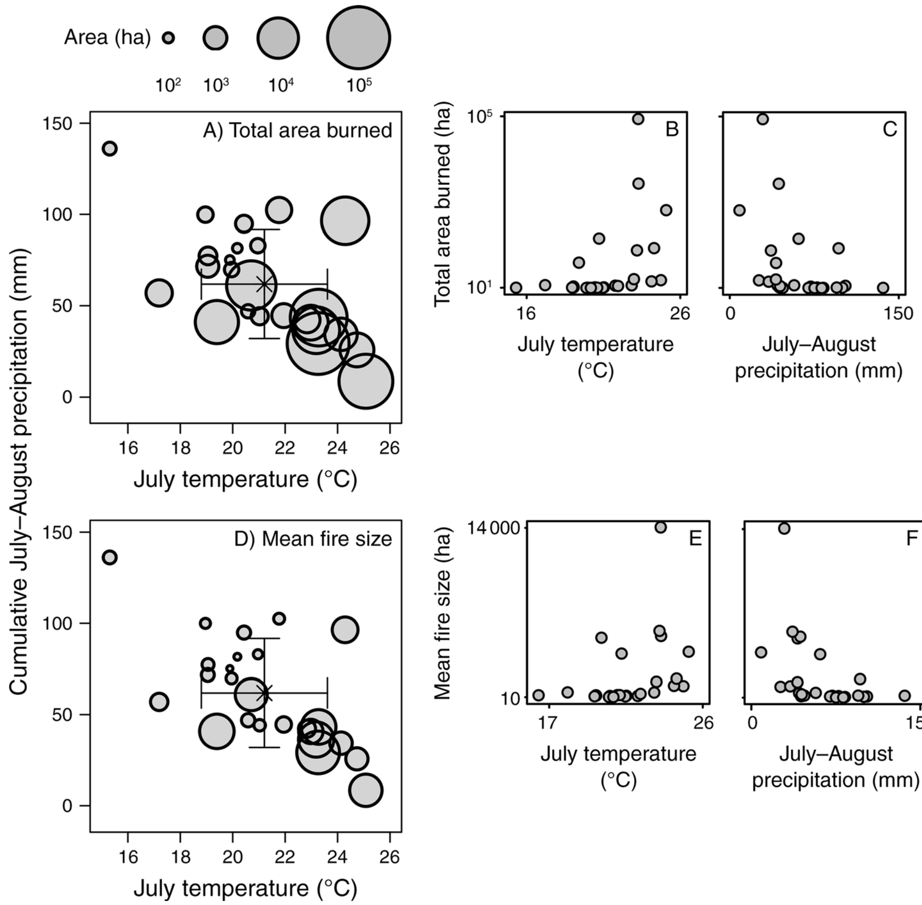

FIG. 2. Scatterplots of July temperature and the total precipitation during July and August, with plot symbols scaled by (A) the total annual area burned (ha) and (D) the annual mean fire size (ha): error bars with X show 25-year mean ± SD for July temperature and cumulative July–August precipitation. Smaller panels on the right are climate variables plotted against untransformed responses of (B, C) annual total area burned and (E, F) annual mean fire size.

Spatial aggregation at the scale of the pixel (two metrics).—Many statistics that assess spatial pattern vary systematically with landscape size (Neel et al. 2004). We used two metrics to measure the aggregation of the high-severity class at the grain of individual pixels that are not correlated with landscape extent: the proportion of like adjacencies (PLADJ) and the Clumpiness Index (CLUMPY). The PLADJ is the number of pixel edges that share an edge with a pixel of the same class, divided by the total number of possible adjacencies. CLUMPY measures the deviation of the PLADJ from that expected under a spatially random distribution.

Statistical analysis.—Simple linear regression was used to test whether fire size was a significant predictor ($\alpha = 0.05$) of within-fire burn-severity pattern. Area measurements (fire size, mean patch size, and area-weighted mean patch size) were $\log_{10}$-transformed for analysis. Mean patch size, area-weighted mean patch size, and Gini coefficients were analyzed for the 120 fires that had high-severity area present. Metrics that assessed pattern at the scale of the pixel were analyzed using data from 116 fires; nine fires (all but one of which were <60 ha) were excluded because they either had no high-severity area present or had a total high-severity area < 0.5 ha (five pixels), rendering those spatial-pattern metrics incalculable. For the Gini coefficient, we fit a nonlinear model because it was theoretically more appropriate, as values for the Gini coefficient should asymptote near its maximum value of 1 and residual plots and visual evaluation indicated that linear models fit the data poorly. To model the proportion of high-severity core area and the PLADJ, an arcsine square-root transformation was applied to the response variable (Kutner et al. 2005). All statistical tests in this study were conducted in the statistical programming language R (R Development Core Team 2010).

RESULTS

Fire and climate

Climate is an important driver of the annual area burned and fire size in the northern Cascade Range. The responses of area burned and fire size were nonlinear,

TABLE 2. Model results for multiple regressions between climate variables and annual area burned, and annual mean fire size for the study area and ecological subsections.

Response variable, by analysis area†	Predictors	F	df	P	R^2‡
Area burned					
Study area§	temp.july** + temp.aug* + temp.june : swe*	10.15	3, 20	<0.001	0.54
Study area¶	tmax.july*** + winter.precip : tmax.sept**	13.56	2, 22	<0.001	0.51
CWF¶	spring.precip : sum.precip*	6.22	1, 17	0.023	0.22
CDF¶ (model 1)	spring.precip + tmax.july + spring.precip : tmax.aug	6.76	3, 10	0.009	0.57
CDF¶ (model 2)	tmax.july* + spring.precip : tmax.aug*	6.84	2, 11	0.012	0.47
WDF¶	winter.precip : tmax.sept*	8.87	1, 8	0.018	0.47
HDW¶	tmax.july* + winter.precip : tmax.june**	7.97	2, 14	0.005	0.47
Mean fire size					
Study area§	temp.july* + sum.precip*	8.91	2, 22	0.001	0.40
Study area¶	sum.precip*** + winter.precip : tmax.june**	13.16	2, 22	<0.001	0.50
CWF¶	spring.precip : sum.precip* + winter.precip : tmax.sept*	7.29	2, 16	0.006	0.41
CDF¶	sum.precip***	21.67	1, 12	0.001	0.61
WDF¶	winter.precip : tmax.sept*	7.71	1, 8	0.024	0.43
HDW¶	winter.precip : tmax.june*	8.25	1, 15	0.012	0.31

Notes: Climate predictor variables for multiple regressions were chosen based on significant univariate predictors and significant interactions ($\alpha = 0.1$) between spring precipitation, winter precipitation, or SWE and other climate variables (Appendix B: Tables B1–B6). Acronyms for climate variables are: swe, 1 May snow water equivalent; winter.precip, spring.precip, and sum.precip, total precipitation October–April, May–June, and July–August, respectively; temp.aug and temp.july, mean temperature for August and July, respectively; tmax.may, tmax.june, tmax.july, tmax.aug, and tmax.sep, average maximum temperature for May, June, July, August, and September, respectively; tdmean.may, tdmean.june, tdmean.july, and tdmean.aug, average dew point temperature for May, June, July, and August, respectively .

* $P < 0.05$; ** $P < 0.01$; *** $P < 0.001$ for significance of individual variables.

† Abbreviations for ecological subsections are as in Table 1.

‡ Adjusted R^2 are provided.

§ COOP and SNOTEL data.

¶ PRISM data.

with drastic increases in annual area burned and fire size in response to warmer and drier climate (Fig. 2). Within the study area, summer climate (July and August temperatures and summer precipitation) explained the most variance and had more significant relationships with area burned and fire size in univariate models. July and August temperatures were highly correlated with summer precipitation, however, probably explaining why one was often dropped from multi-predictor models. We found significant positive relationships between temperature and negative relationships between SWE (snow water equivalent) or precipitation and both the area burned and fire size (Table 2; Appendix B: Tables B1–B6). Antecedent climate (spring SWE, winter and spring precipitation) was equally significant in many models, but slopes for antecedent climate variables were less steep and less variance was explained compared to summer season variable models. Summer temperature, particularly July temperature, and the interaction between winter precipitation (SWE or rainfall) and late-summer temperature (August or September) were significant predictors in the models predicting area burned for the study area and individual subsections (Table 2). Summer (study area, CWF, CDF) or winter (study area, CWF, HDW, WDF) precipitation were consistently significant predictors of mean fire size (Table 2).

Fire size and burn severity

Burn severity reflected differences in fire regimes within the study area. Over the whole study area, 316 567 ha, or 22% of the study area, burned during the study period, and 41% of that area burned with high severity (Table 3). High and moderate severity constituted most of the area burned, in all subsections except the CWF (Table 3). The HDW had more moderate

TABLE 3. Burn severity by ecological subsection.

Analysis area	No. fires	Total area burned (ha)†	Area burned, by severity (ha)‡			
			High	Moderate	Low	Unchanged
Study area	125	316 567 (22%)	129 238 (41%)	84 181 (27%)	46 041 (15%)	55 720 (18%)
CWF	51	9541 (2%)	2329 (25%)	2569 (27%)	1696 (18%)	2896 (31%)
CDF	32	155 211 (44%)	80 972 (53%)	34 625 (22%)	18 725 (12%)	19 593 (13%)
WDF	12	46 078 (27%)	16 050 (35%)	13 552 (29%)	7125 (15%)	9353 (20%)
HDW	30	105 737 (32%)	29 887 (28%)	33 435 (32%)	18 495 (17%)	23 878 (23%)

† Percentage of subsection or study area is shown in parentheses.

‡ Percentage of total area burned at a given severity is shown in parentheses.

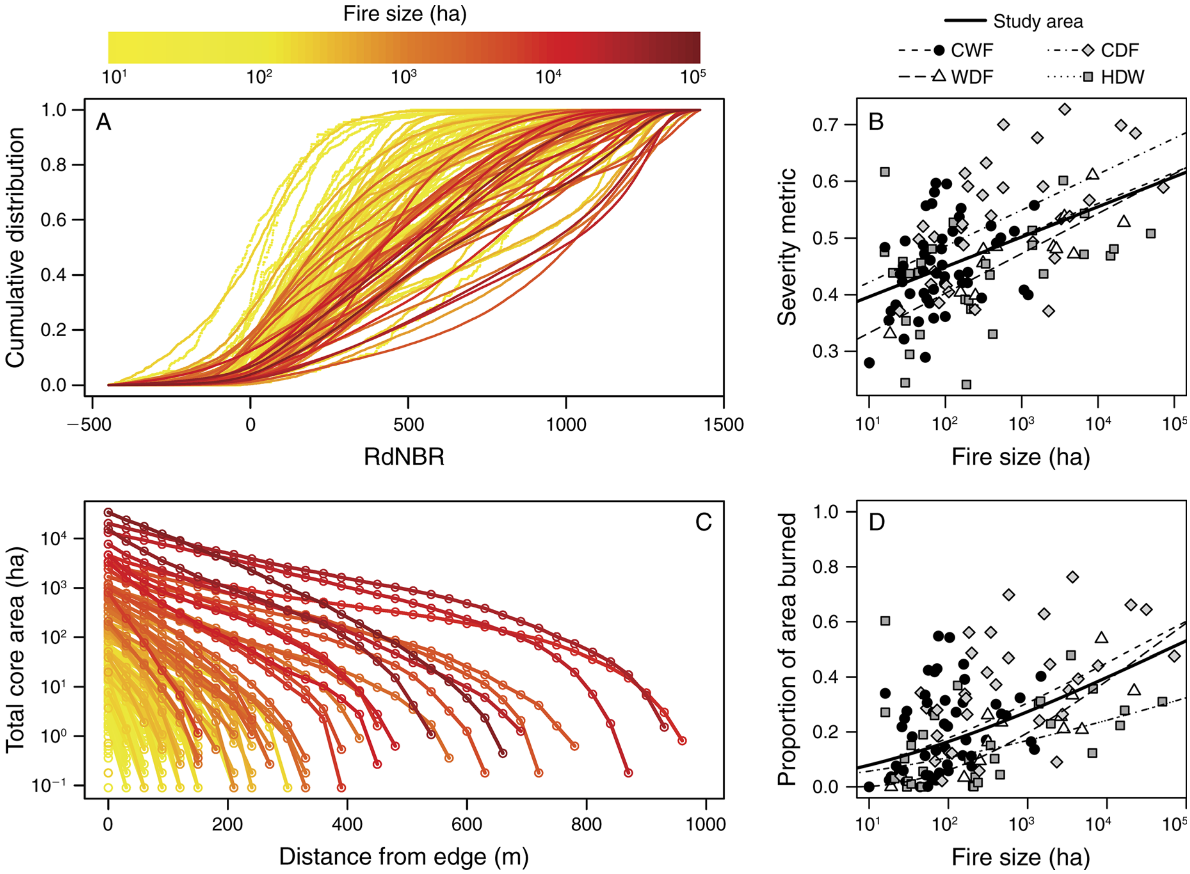

FIG. 3. (A) Cumulative distribution of the RdNBR (Relative differenced Normalized Burn Ratio) for all 125 fires > 10 ha that burned between 1984 and 2008. RdNBR is a spectral burn-severity index based on the near- and mid-infrared portions of the electromagnetic spectrum. Each distribution is colored according to the size of the fire. Fires that burned with higher severity have a slower increase in their cumulative distribution, and less area under the cumulative distribution curve. This is quantified by the severity metric (SM). (B) A scatterplot and linear regressions of fire size and the SM, showing a significant increase in severity with fire size for the study area and all ecological subsections except HDW (see Fig. 1 for locations: CWF, Cool Wet Temperate and Subalpine Forests; CDF, Cold Dry Montane and Subalpine Forests; WDF, Warm Dry Mixed-Conifer Forests; HDW, Hot Dry Woodland and Steppe). (C) Total high-severity core area in each fire, when core area is defined by a specific distance from the edge of the patch (shown here in 1 pixel/30 m increments). Lines represent individual fires, and are colored according to the size of the fire. (D) Scatterplots and significant linear regression equations for the proportion of area burned at high severity as a function of fire size, for the study area and each subsection. Only statistically significantly regressions ($P < 0.05$) are shown.

severity than high severity, whereas the CDF and WDF burned predominantly with high severity. The CDF had largest total area burned (155 211 ha, or 44% of the subsection) and the greatest percentage of high severity (53% of the area burned in the subsection) of the four subsections, but had relatively less area burned at moderate severity (Table 3).

Burn severity increased with fire size. The cumulative distributions of the RdNBR for each of the 125 fires (Fig. 3A) demonstrate that the larger fires (red colors) have a greater proportion of their pixels in high RdNBR values. Some are even concave-up (i.e., no inflection point), whereas smaller fires (yellow colors) have sigmoidal cumulative distributions, indicating a higher proportion of the pixels in lower RdNBR values. The SM, which quantifies these curves, significantly increases with fire size at the extent of the study area ($R^2 = 0.23$, $P = <0.001$) and in all subsections except the HDW (Table 4, Fig. 3C). The proportion of the area burned at high severity increased as fire size increased at the scale of the study area ($R^2 = 0.22$, $P < 0.001$) and in all subsections (Fig. 3D), and the proportion of area where no change was detected decreased as fire size increased across the study area ($R^2 = 0.19$, $P < 0.001$) and in all subsections except the HDW (Table 4).

Fire size and burn-severity pattern

Patch size.—At the extent of the study area, high-severity mean patch size and area-weighted mean patch size both increased significantly with fire size (Table 5). The relationship between fire size and area-weighted mean patch size followed a power-law distribution (Fig. 4). Within the subsections, high-severity mean patch size increased significantly with fire size only in the CDF

TABLE 4. Regression models predicting the severity metric (SM) and proportion of area burned at a given severity as a function of fire size, for the whole study area and for each subsection.

Burn severity, by analysis area	Slope (SE)	P	Adjusted R^2
Severity metric (RdNBR)			
Study area	0.11 (0.02)	<0.001	0.23
CWF	0.11 (0.04)	0.009	0.11
CDF	0.13 (0.04)	0.001	0.28
WDF	0.14 (0.03)	<0.001	0.70
HDW	0.06 (0.03)	0.063	0.09
High			
Study area	0.27 (0.04)	<0.001	0.22
CWF	0.30 (0.12)	0.012	0.10
CDF	0.30 (0.08)	0.001	0.28
WDF	0.42 (0.08)	<0.001	0.70
HDW	0.18 (0.08)	0.036	0.12
Moderate			
Study area	0.02 (0.02)	0.368	0.00
CWF	0.11 (0.06)	0.073	0.04
CDF	−0.07 (0.03)	0.019	0.14
WDF	0.10 (0.05)	0.091	0.18
HDW	0.06 (0.06)	0.383	−0.01
Low			
Study area	−0.05 (0.02)	0.009	0.05
CWF	−0.02 (0.04)	0.662	−0.02
CDF	−0.09 (0.03)	0.008	0.19
WDF	−0.17 (0.04)	0.002	0.60
HDW	−0.02 (0.04)	0.589	−0.02
No change detected			
Study area	−0.19 (0.03)	<0.001	0.19
CWF	−0.28 (0.09)	0.003	0.15
CDF	−0.17 (0.06)	0.007	0.19
WDF	−0.23 (0.05)	0.002	0.61
HDW	−0.12 (0.08)	0.152	0.04

Notes: The SM was calculated following Lutz et al. (2011) using continuous RdNBR (Relative differenced Normalized Burn Ratio) images clipped to the boundary of each fire, and modeled as $y = b_0 + b_1(\log_{10}(\mathrm{TA}))$; higher values of the SM indicate increased burn severity. For the percentage of area at a given severity class, models are also in the form: $y = b_0 + b_1(\log_{10}(\mathrm{TA}))$, where TA is total area of the fire. The SM and proportions were arcsine square-root transformed before analysis (Kutner et al. 2005).

(Table 5, Fig. 4A). High-severity area-weighted mean patch size increased significantly with fire size in all subsections, but more variance was explained in the CDF and WDF ($R^2 = 0.75$, $P < 0.001$ and 0.73, $P < 0.001$, respectively), than in the CWF or HDW ($R^2 = 0.38$, $P < 0.001$ and $R^2 = 0.49$, $P < 0.001$, respectively). Regression for area-weighted mean patch size explained much more of the variance than the regression between fire size and mean patch size (Table 5), meaning that the patch size in which a randomly selected pixel is likely to be located increased more with fire size than did the size of a randomly selected patch.

Patch-size distributions reflected the size of fires in the subsection and the proportion of area burned at high severity (Appendix B: Fig. B1, Table B7). In the CDF, which had the largest fires and greatest proportion of high severity, a large percentage of the area burned (37%) was within high-severity patches larger than 10^3 ha. In the CWF, which had the lowest total area burned and smaller fires, most of the area that burned at high severity was in patches of 10–10^3 ha. When calculated across high-severity patch distributions aggregated over all fires in a subsection, area-weighted mean patch sizes were highest in the CDF (7335 ha), followed by the WDF (807 ha), the HDW (110 ha), and lowest in the CWF (15 ha) (Appendix B: Table B7).

Size inequality.—The size inequality of high-severity patches, as measured by the Gini coefficient, increased with fire sizes both at the scale of the study area and within each subsection (Fig. 4C). Nonlinear models explained 56% of the variance at the scale of the study area, and 49%, 71%, 50%, and 45% of the variance in the CWF, CDF, WDF, and HDW, respectively (based on pseudo-R^2; Appendix B: Tables B8–B12). The parameters of the nonlinear models were highly significant at the scale of the study area and in the CDF, but were not always significant at $\alpha = 0.05$ in other subsections (especially CWF). Nevertheless, residual plots and visual examination of scatterplots indicated that nonlinear models were appropriate, whereas linear models poorly fit the data, despite having $R^2 > 0.44$ and $P < 0.001$ in each analysis area (not shown). When calculated across high-severity patch distributions aggregated over all fires within a given size class, the Gini coefficients were higher in the larger fire size classes, and highest in the CDF (0.97), followed by the WDF (0.93), the HDW (0.91), and lowest in the CWF (0.88) (Appendix B: Table B7).

Patch interior.—The proportion of high-severity core area increased significantly with fire size across the study area ($R^2 = 0.38$, $P < 0.001$) and within all subsections (Table 5, Fig. 4D). The increase was greater and more variance was explained in the CDF and WDF than the CWF and HDW (Table 5). In our post hoc sensitivity analysis testing definitions of core area ranging from 30 m to 300 m, regressions at the scale of the study area explained 27% to 47% of the variance and were consistently significant at the $P < 0.001$ level (Appendix B: Figs. B2 and B3).

Larger fires had more total core area across all definitions of core area (0–990 m in from patch edge) and had high-severity core area present at much greater distances from patch edges than did smaller fires (Fig. 3C). The relationship between core area and fire size was not absolute. The amount of high-severity core area in some of the largest fires dropped off at larger edge depths (>500 m), but three fires (the third, fifth, and eighth largest fires, of sizes 31 340, 20 070, and 8533 ha, respectively) had high-severity area >800 m in from patch edges.

Spatial aggregation at the scale of the pixel.—Over the entire study area, the PLADJ increased with fire size (Table 5, Fig. 4E), but no significant relationship with fire size was apparent when spatial aggregation was measured with CLUMPY ($P = 0.057$). There was a significant increase in the PLADJ in all subsections

TABLE 5. Regression models predicting spatial-pattern metrics for high severity as a function of fire size at the extent of each ecological subsection.

Spatial-pattern metric by analysis area	Slope (SE)	F	df	P	R^2
Mean patch size					
Study area	0.19 (0.06)	11.78	1, 114	<0.001	0.09
CWF	0.25 (0.15)	2.73	1, 45	0.105	0.04
CDF	0.27 (0.1)	7.78	1, 30	0.009	0.18
WDF	0.21 (0.17)	1.43	1, 9	0.263	0.04
HDW	0.14 (0.11)	1.72	1, 24	0.202	0.03
Area-weighted mean patch size					
Study area	0.99 (0.07)	179.80	1, 114	<0.001	0.61
CWF	0.89 (0.17)	28.86	1, 45	<0.001	0.38
CDF	1.16 (0.12)	94.97	1, 30	<0.001	0.75
WDF	1.07 (0.2)	28.39	1, 9	<0.001	0.73
HDW	0.86 (0.17)	25.43	1, 24	<0.001	0.49
Gini coefficient					
Study area	0.19 (0.02)	96.25	1, 114	<0.001	0.45
CWF	0.31 (0.05)	36.56	1, 45	<0.001	0.44
CDF	0.15 (0.03)	33.04	1, 30	<0.001	0.51
WDF	0.11 (0.03)	14.50	1, 9	0.004	0.57
HDW	0.21 (0.05)	21.66	1, 24	<0.001	0.45
Proportion of total area burned >90 m from patch edge (core area)					
Study area	0.25 (0.03)	70.67	1, 114	<0.001	0.38
CWF	0.22 (0.07)	10.06	1, 45	0.003	0.16
CDF	0.35 (0.06)	29.02	1, 30	<0.001	0.47
WDF	0.27 (0.10)	7.86	1, 9	0.021	0.41
HDW	0.15 (0.04)	11.97	1, 24	0.002	0.30
Proportion of like-adjacencies					
Study area	0.22 (0.04)	25.98	1, 114	<0.001	0.18
CWF	0.27 (0.1)	7.73	1, 45	0.008	0.13
CDF	0.25 (0.07)	13.81	1, 30	<0.001	0.29
WDF	0.21 (0.11)	3.72	1, 9	0.086	0.21
HDW	0.23 (0.11)	4.37	1, 24	0.047	0.12
Clumpiness index					
Study area	0.03 (0.02)	3.71	1, 114	0.057	0.02
CWF	0.01 (0.03)	0.14	1, 45	0.713	−0.02
CDF	0.05 (0.03)	3.82	1, 30	0.060	0.08
WDF	0.03 (0.05)	0.46	1, 9	0.513	−0.06
HDW	0.06 (0.05)	1.40	1, 24	0.248	0.02

Notes: Spatial-pattern metrics were modeled with a simple linear regression following the form: $y = b_0 + b_1(\mathrm{TA})$, where TA is the total area of the fire. Proportions were arcsine square-root transformed before analysis (Kutner et al. 2005). Area measurements (total area of the fire, mean patch size, and area-weighted mean patch size) were $\log_{10}$-transformed before analysis. Results for nonlinear models for Gini coefficient are present in the text and Appendix B: Tables B8–B12.

except for the WDF, but none of the regressions between CLUMPY and fire size were significant (Table 5, Fig. 4F). Therefore the significant relationships between fire size and the PLADJ were due to the increased proportion of area burned at high severity in larger fires.

Discussion

Fire and climate

The larger climate patterns experienced in the northern Cascade Range facilitate interpretation of the climate variables found to be significant predictors. Whereas in many regions in the western USA the fire season consistently starts by July, conditions in the CWF may stay or become cool and wet even in the middle of the summer. Therefore the flammability of fuels across the landscape is limited not only by spring climate, but also by summer temperature and precipitation. This differs from the HDW, where fuels almost always become dry enough during the summer to burn. In these areas, winter and spring climate, particularly winter precipitation and the temperatures at the beginning and end of the fire season, influence the overall length of the fire season and production of fine fuels, and therefore are more clearly associated with annual area burned and fire size. These results suggest that the importance of climate variables in controlling area burned and fire size is contingent. Adequate conditions for burning during the summer first need to be met before variation in the length of the fire season becomes important.

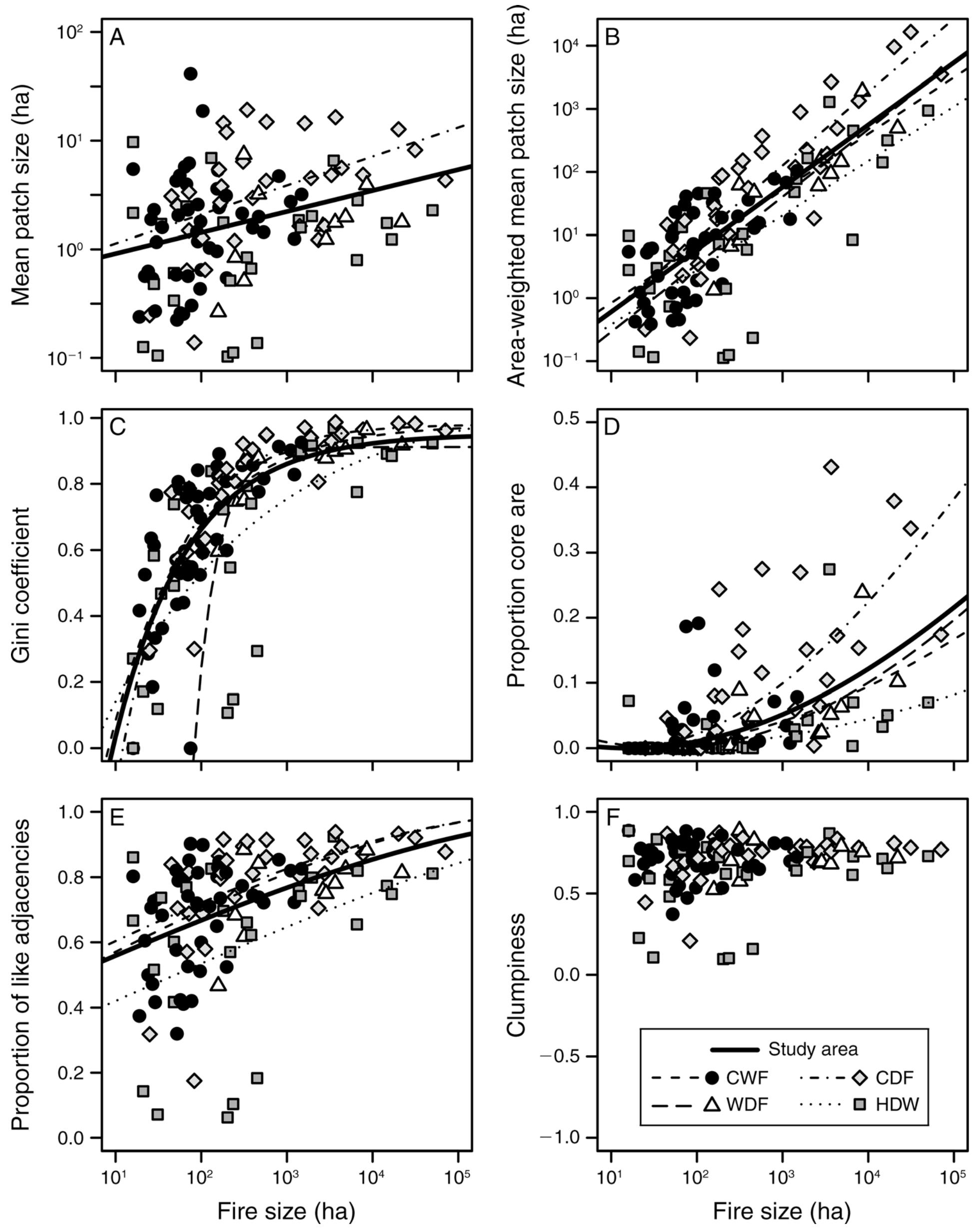

FIG. 4. Scatterplots and regression equations for fire size and (A) mean high-severity patch size; (B) area-weighted mean high-severity patch size; (C) Gini coefficient for high-severity patches; (D) the proportion of the total area burned made up of high-severity core area (where core area is defined as being >90 m from a patch edge); (E) the proportion of like adjacencies (PLADJ); and (F) the high-severity Clumpiness index (CLUMPY). Only statistically significantly regressions ($\alpha = 0.05$) are shown. Area-weighted mean patch size weights each patch by its size, reflecting the patch size in which a randomly chosen pixel would most likely be found; like mean patch size, it provides an absolute measure of patch size. The Gini coefficient measures the size inequality of the patch distribution relative to minimum and maximum patch sizes observed, and measures patch size relative to fire size, allowing comparisons among fires of different sizes, with different maximum possible patch sizes. PLADJ and CLUMPY measure the aggregation of the high-severity class at the grain of individual pixels. PLADJ is the number of pixel edges that share an edge with a pixel of the same class, divided by the total number of possible adjacencies. CLUMPY measures the deviation of the PLADJ from that expected under a spatially random distribution, given the proportional cover of the high-severity class.

Although contemporary relationships between climate and area burned have been used to project future changes (Littell et al. 2010, Wotton et al. 2010), these relationships may not be stationary under future climate. In the Pacific Northwest, climate models project increases in annual mean temperatures and possible increases in annual precipitation, but decreases in summer precipitation and relatively larger increases in summer temperatures (Mote and Salathé 2010). If summer climate in the northern Cascade Range changes so that thresholds for burning are always reached during the summer, a shift in the specific climate factors that constrain area burned may occur. Climate variables such as spring SWE that are related to the start of the fire season may become more important drivers of annual area burned and fire size. The strength of the relationships between climate and the annual area burned and fire size in the future will also be mediated by the extent to which previous disturbances decrease the probability or severity of subsequent disturbance (Peterson 2002, Moritz et al. 2011). Uncertainty arises from lack of knowledge of whether fire regimes in which previous fires currently inhibit the spread of subsequent fires will continue to exhibit this trait under future climate (McKenzie and Littell 2011).

Translating observed increases in area burned to landscape effects

In the northern Cascade Range, larger fires created a more homogeneous landscape pattern by increasing patch sizes while reducing the proportion of the landscape in low and moderate severity. Burn severity and high-severity patch size, patch size inequalities, patch interior, and spatial aggregation of high-severity pixels were positively correlated with fire size. Our results correspond with significant relationships between fire size or area burned and burn severity and high-severity patch size in the Sierra Nevada (Lutz et al. 2009, Miller et al. 2009*b*, 2012*a*, *b*), and between area burned and burn severity in the Rocky Mountains (Dillon et al. 2011).

Despite the increasing evidence that increases in fire size and area burned correspond with increases in severity and larger, more homogenous high-severity patches, large fires should not simply be seen as ecological catastrophes (Keane et al. 2008). In our study area, large fires created more *total* area in smaller patch sizes than smaller fires did, even though larger patches made up a greater *proportion* of the area within large fires. Fires > 10 000 ha probably maintained the heterogeneity of 151 072 ha that were outside large (>100 ha) patches of high severity. This amounts to over 47.7% of the total are burned in the study area, and is twice as much area as the area outside of large patches burned by fires < 10 000 ha (71 531 ha). Therefore, within a least part of the area burned by large fires, landscape heterogeneity has increased, whereas in other portions, large homogenous patches were created.

We found little support for the idea that differences in fire suppression policies were influencing area burned or burn-severity patterns. Unlike many other large wilderness complexes, fires are actively suppressed in the majority of wilderness areas within our study area. Wildland fire use is permitted within the boundaries of North Cascades National Park Complex, which makes up ~18% of our total study area, almost entirely within the CWF. Unlike other wilderness areas with wildland fire use policies in places, where previous fires have been shown to limit the spread or severity of subsequent fires (Collins et al. 2009, Lutz et al. 2009, Teske et al. 2012, Parks et al. 2014; but see Haire et al. 2013), fires in the CWF seem to be limited in size by the cool wet climate and limited fuel connectivity, as seen by their small size and spatial isolation (Fig. 1). We did not examine differences between wilderness and non-wilderness in other parts of our study area, as any differences most likely would be due to ecological differences: most of the wilderness is higher in elevation, with different forest types and different fire regimes, which are already captured within the different subsections.

Differences in fire regimes between the subsections directly reflect their differences in vegetation, topography, and climate. The strongest relationship between fire size and the spatial aggregation of high severity was in the CDF, reflecting connected forests of fire-intolerant tree species, few barriers to fire spread, and weather during the large fires. In this subsection, extreme fire weather and dry climate did seem to override local controls (sensu Turner and Romme 1994, Bessie and Johnson 1995), but that occurred within a context of a biophysical setting with weak "bottom-up" controls. In the CWF, the smaller fire sizes, smaller patch sizes, less core area, more equal patch-size distributions, and greater spatial complexity, relative to other subsections, reflected the constraints of complex topography, higher fuel moistures, and nonflammable areas on fire behavior and spread. In the HDW, the topography is relatively simple, but the fine-grain mosaics of vegetation and stand structure in low- and mid-elevation forest acted as strong local controls that keep weather from having an overriding influence on fire behavior (Agee 1997).

Our results provide the basis for the conceptual model presented in Fig. 5, in which the relationship between fire size and spatial pattern of severity is mediated by two main factors: (1) the severity of the fire regime, and (2) the strength of local "bottom-up" controls. Local controls include topographical barriers to fire spread, the variability or "complexity" of topography, and the spatial complexity of vegetation and fuels. In active low-severity fire regimes, fuel limitations and adaptive traits of the vegetation may limit the occurrence of high burn severity, even when fires are large. In mixed- and high-severity fire regimes, fuels are not limiting and the full range of severity can be expressed (Agee 1997). The spatial complexity and configuration of fuels is influenced by feedbacks from previous disturbances, temporal variation in climate, and topography. In areas with complex topography or greater spatial variability in vegetation and fuels, climate and weather are less likely to override those local "bottom-up" controls (Kennedy and McKenzie 2010, McKenzie and Kennedy 2012), which constrain fire behavior and the creation of large, homogeneous high-severity patches. In these areas, instead of "overriding" or removing the influence of fuels and topography, climate may increase the spatial

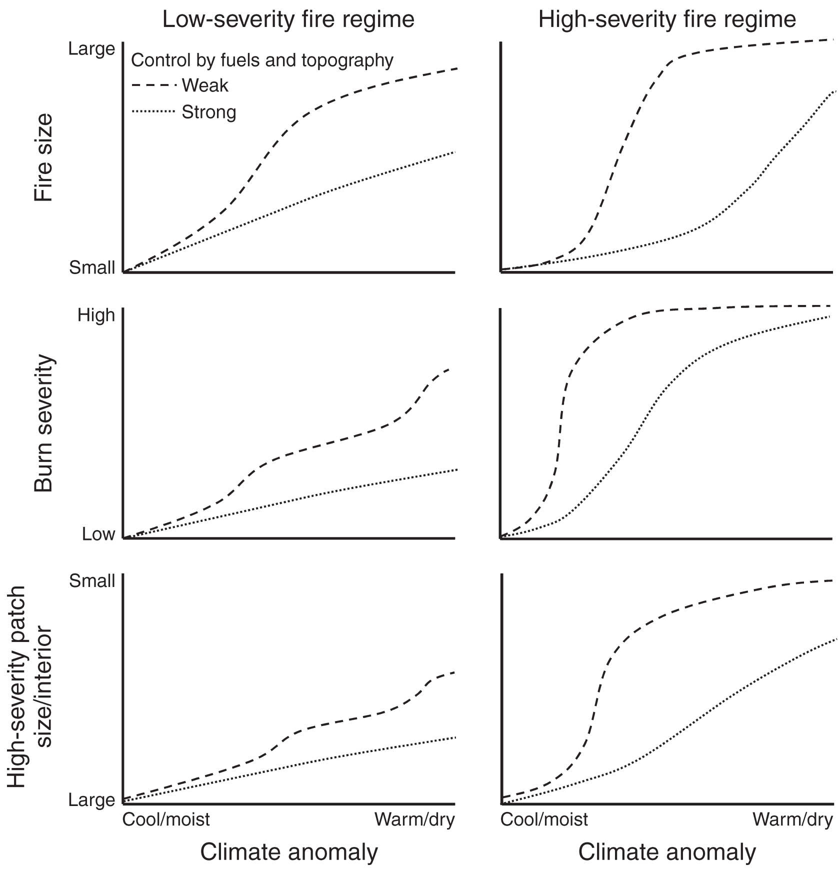

FIG. 5. Conceptual diagram of theoretical constraints imposed by (1) the severity of the fire regime and (2) the strength of local endogenous controls (i.e., fuels and topography) on the relationship between climate and fire-regime attributes (fire size, burn severity, and the size of high-severity patches). Lines represent the aggregate properties of multiple fires over time, as opposed to individual events. We hypothesize that in systems with weak endogenous controls, nonlinear changes in fire-regime attributes are more likely. In high-severity fire regimes, this is reflected in sudden and marked increases in fire size and severity, and the creation of extremely large high-severity patches. In lower-severity fire regimes, this may be reflected in simply a faster increase in fire size, severity, and high-severity patch size in areas with weak local controls, or as shown here for fire severity and high-severity patch size, a step-like increase.

grain at which those local controls influence burn-severity pattern.

An important question put forth by our conceptual model (Fig. 5) is how "top-down" climatic controls, the severity of fire regimes, and variation in drivers at local and meso scales interact to create linear or nonlinear changes in the emergent properties of fire regimes. Statistically significant relationships between fire size and burn severity are found in some regions—interior Alaska (Duffy et al. 2007), the northern Rocky Mountains (Keane et al. 2008, Dillon et al. 2011), Southern Rockies (Dillon et al. 2011), the Sierra Nevada, and southern Cascade Range (Lutz et al. 2009, Miller et al. 2012*a*)—but not others (Pacific Northwest, Inland Northwest, Colorado Plateau, and Mogollon Rim; Dillon et al. 2011). Although these results may be due, in part, to differing methodologies among studies, as we will discuss, across the larger-scale variation in the western USA they agree with our model. Stronger relationships between area burned and severity are present in higher-severity fire regimes, such as more continuous mixed-conifer and subalpine forests in the northern Rocky Mountains and the Sierra Nevada. Regions where significant relationships have not been detected, such as the Inland Northwest or southwestern USA, have lower-severity fire regimes and more heterogeneous fuels, indicative of *Pinus ponderosa* and mixed-conifer forests.

As with climate–fire size relationships, the relationship between fire size and severity and the spatial pattern of burn severity may not remain stationary under a future climate. If the relationship between fire size and severity is nonlinear, then thresholds associated with climate may be reached after which the emergent properties of fire regimes shift suddenly. Other factors may either ameliorate or exacerbate the homogenizing influence of increased severity and increased high-severity patch size. The cumulative impacts of increases in the fire size, severity, and high-severity patch size and patch interior on the long-term landscape pattern will depend on feedbacks from future processes, including availability of seed sources, spatial variability of vegetation recovery within large high-severity patches, and future disturbances. For example, the 90-m distance that we used to define core area corresponds to the distances within which >90% of wind-dispersed seeds of many temperate conifer species fall (McCaughey et al. 1986). Early-successional vegetation may persist for a long time within large patches with a substantial core area due to limitation to seed dispersal from the edge of patches (Donato et al. 2009, Haire and McGarigal 2010), although high winds, steep relief, and dispersal by bird and mammal species (Vander Wall 2008, Lorenz et al. 2011) make it likely that some seed dispersal occurs far from seed sources. Persistence of early-successional habitats on the landscape will benefit a diverse assemblage of early-successional obligate species (Swanson et al. 2011), but corresponding decreases in late-successional habitat and complicated intermixes of habitat types would have negative impacts on species that depend on late-successional habitat (McKenzie et al. 2004). With the creation of large high-severity patches and limitations on regeneration caused by shifts in climate, these large patches may change to novel species assemblages or from forest to non-forest (Brubaker 1986, Savage and Mast 2005, Bowman et al. 2013). On the other hand, heterogeneity in topography, soils, and water availability may diversify species composition and successional rates, even within large high-severity patches (Savage et al. 2013). The relative importance of variation in disturbance severity compared to spatial variance in successional processes on landscape pattern is unknown for most ecosystems, and research on how these two processes interact will be key to understanding the cumulative effects of climate change on landscape pattern.

Fire extent and severity, and prevalence of large, homogeneous high-severity patches, will also be affected by future disturbances. More disturbance could move vegetation community and structure to alternative stable states (Westerling et al. 2011, Bowman et al. 2013) or alternatively could restore resilience to landscape structure and function (Larson et al. 2013), depending on how much the severity or frequency of fires departs from those of current and historical fire regimes, and the taxa involved. Subsequent fires may reinforce homogeneous patterns created by past disturbances, or create new, more heterogeneous, patterns. In some mixed-severity or low-severity fire regimes, where fire suppression has increased the horizontal and vertical continuity of fuels (Hessburg et al. 2005), large patches of high severity may facilitate postfire establishment of flammable shrub species (e.g., *Arctostaphylos*, *Ceanothus*) that are likely to re-burn with high severity (Perry et al. 2011) and maintain a new stable state. Conversely, previous fires may limit the spread of future fires (Peterson 2002, Collins et al. 2009, Teske et al. 2012). For example, in the CDF, previous burns and fuel treatments that include prescribed fire effectively decrease the severity of subsequent fires, and therefore contribute to a heterogeneous burn-severity pattern, even under extreme weather (Lyons-Tinsley and Peterson 2012, Prichard and Kennedy 2012). Little area re-burned in our study area (approximately 2% of the total area burned was burned twice or more during the 25-year study period; Cansler 2011), but in other regions with active wildland fire-use programs, re-burns were less severe (Miller et al. 2012*b*, Parks et al. 2014) and exhibited more complex spatial patterns (Collins and Stephens 2010, Miller et al. 2012*b*, Teske 2012).

Spatial scale influences analysis of burn-severity pattern

Remotely sensed burn-severity data, such as those used in this study, are now readily available for much of North America, facilitating analyses at spatial scales from individual fires to regions. Because ecological processes vary across scales (Levin 1992), and contagious disturbances such as fire are constrained by characteristic scales of landscape spatial structure (McKenzie and Kennedy 2011), the associated scales of ecological inferences are bounded. For example, fire-size distributions can be quantified statistically only if the geographic domain is large enough to capture extreme events, but not so large that it encompasses widely different bioclimatic zones (Moritz et al. 2011). Consequently, the scale of the data used can either facilitate or confound inferences. If the scales of design and inference are matched, we suggest that the former will ensue. In analyses such as this one, important design considerations include the minimum fire size cutoff, the ecological variation within vs. among the study areas, and the particular metrics used to quantify the burn-severity pattern. Each of these reflects a different dimension of scale compatibility.

Issues of scale regarding the minimum fire size and the extent of the study area may compromise the ability to detect significant relationships between fire size and burn severity or high-severity patch size. For example, the domain assessed by Dillon et al. (2011), the Inland Northwest ecoregions, includes our study area but is an order of magnitude larger. We found a significant increase in burn severity, whereas they did not. Differences are not due to our use of fire size instead of annual area burned (as they did) as a predictor. If we regress the proportion of annual area burned at high severity as a function of annual area burned, our results remain significant ($P < 0.001$) and have even greater explanatory power ($R^2 = 0.39$). (See Miller et al. [2012*b*] for an example of how the scale at which area burned data is aggregated—by fire or by year—may influence results.) Therefore, we suggest that the difference between our study and that of Dillon et al. (2011) is because they used a higher minimum fire size cutoff (400 ha, following that of the MTBS program), thereby excluding area burned by smaller, less severe fires, or because their geographic domain included areas where there were significant positive relationships between burn severity and area burned (i.e., the northern Cascade Range), and areas where the relationship was negative or neutral, or both. If we predict percentage of high severity as a function of area burned using only data from fires > 400 ha ($n = 14$ years) the regression is only marginally significant at $\alpha = 0.05$ and explains less variance ($R^2 = 0.24$, $P = 0.044$). Fires < 400 ha are still ecologically important in the complex terrain of the West, and attributes of fire regimes can vary over relatively small spatial scales (10–100 km), due to the flammability and fire tolerance of the vegetation and steep environmental gradients. All of these examples imply that aggregating models, from individual fires to small regions, must be done with care. Investigating relationships between drivers and severity and spatial pattern of fire using a nested hierarchy of geographical extents may be necessary to identify the appropriate geographic and ecological domain of the relationships.

Although many metrics measure spatial pattern, some may be more sensitive to specific types of changes than others (Cushman et al. 2008), and therefore studies should ideally measure pattern using a variety of metrics. Our study and others have found that metrics that measure patch size or patch interior are more strongly correlated with area burned than finer-scale metrics based on pixel adjacencies (Keane et al. 2008, Haire and McGarigal 2009, Miller et al. 2012*a*). This may be because they are more sensitive to continuous aggregation of a severity class over distances greater than that of 1 pixel (i.e., matched to the spatial scale of landscape fire dynamics). Metrics based on pixel adjacency may also be more difficult to translate to definitive ecological effects. For example, the same PLADJ could represent all pixels having one neighbor, or a mix of pixels having all four neighbors (possibly within very large patches) and pixels with fewer or no neighbors (i.e., in very small patches). Because many of the ecological effects of the burn-severity pattern, such as seed dispersal, take place over a distance greater than 30 m (1 pixel), we suggest that patch-based metrics and measures of patch interior or distance to edge are not only at the appropriate scale for analysis, but also are more informative to other scientists and to managers.

Management implications

Our results show that severity and spatial attributes of fire regimes in the northern Cascade Range depend on fire size and the climatic variables that are correlated with fire-size distributions. In the Pacific Northwest, the climate associated with greater area burned and larger fire sizes, and therefore associated with the formation of large, high-severity patches, is projected to become more common in the future (Littell et al. 2010, Mote and Salathé 2010). If the statistical relationships found here between climate, fire size, severity, and burn-severity pattern persist under future climate, the landscapes of the future may be very different from the landscape today. Increases in the size, severity, and homogeneity of the spatial pattern of fires probably would increase the proportion of the landscape in homogeneous early-successional patches, and potentially would decrease beta diversity (sensu Whittaker 1960) and ecological resilience (Holling 1973, van Nes and Scheffer 2005) across the landscape.

These changes in fire regimes and landscape pattern would affect a variety of other ecosystem process, including belowground processes (Neary et al. 1999), hydrology and geomorphology (Swanson 1981), and carbon storage (Meigs et al. 2009, Raymond and McKenzie 2012). Burn severity and burn-severity pattern affect a wide variety of wildlife species (Roberts et al. 2008, Wightman et al. 2010, Dudley et al. 2012, Buchalski et al. 2013). Accordingly, understanding how changes in fire regimes and their impacts on landscape composition and pattern affect these species should be a major focus for future research.

Ideally, maintaining resilient landscapes provides a buffer against abrupt changes in landscape pattern and process in response to rapid climate change. Adaptive management to increase resilience includes mechanical treatments and prescribed fire, both for fuel reduction and to maintain heterogeneous stand structures, designed at spatial scales that match patch-size distributions expected under changing fire regimes (Peterson et al. 2011, Prichard and Kennedy 2012). An alternative to managing to restore historical reference conditions associated with past (e.g., Little Ice Age) climate is using "climate analog reference conditions" (Churchill et al. 2013) that anticipate new disturbance regimes associated with future projections of climate (Littell et al. 2010).

In arid mountain landscapes of the Pacific Northwest (i.e., east of the Cascade crest), spatial heterogeneity of vegetation, patch sizes, and fire severity was widespread historically (Hessburg et al. 2005, 2007). Fire-size distributions reflected characteristic spatial scales of landforms, and therefore the spatial patterns of vegetation (fuels) that provided endogenous controls on all but the most extreme wildfires. We suggest that there may be a spatial hierarchy of endogenous controls that limit fire spread and behavior, ranging from variation within stands, particularly in low- and mixed-severity regimes (Larson and Churchill 2012), at the scale of local topography (Lydersen and North 2012), and at larger scales that reflect the influence of topography on local weather (e.g., diurnal canyon winds) and of variation in stand ages due to past disturbances. In a warming climate, with the larger high-severity patches associated with larger fires that our results suggest, there may be an increase in scale of the "relevant" endogenous controls, with larger-scale controls playing a more important role controlling fire spread and behavior. To promote resilience, one might try to create spatial heterogeneity at the future "relevant" scales under climate change. The problem is that we are uncertain about what this scale is (although we expect that it will be larger). Therefore, we suggest that endogenous controls on fire might be best supported by maintaining spatial heterogeneity at multiple scales. Aiming for spatial heterogeneity across scales has the further advantage of maintaining options, in the form of landscape variability, in the face of extreme events, a strategy held to be robust, or "anti-fragile" (Taleb 2012) in a wider range of applications that includes protecting against natural hazards or economic failures.

With changes in fire regimes likely to be inevitable, actions to protect specific resources will take advantage of place-specific or scale-specific strategies. For example, increased use of wildfires to achieve resource objectives (van Wagtendonk and Lutz 2007, Hunter et al. 2011, Miller et al. 2012*b*, North et al. 2012, Haire et al. 2013), as has been implemented in the CWF within North Cascades National Park Complex, may be the only logistically feasible method for maintaining valued resources such as wildlife and water quality. Allowing wildfires to burn for resource benefit may be implemented with the least risk during years with mild climate, which probably would have the added benefits of burning with lower severity and more spatial heterogeneity. Other more specific actions include altering road infrastructure so that it is less vulnerable to erosion, removing nonnative species so that native communities can reestablish after high-severity fire, and incorporating future climate to determine the density, species, and genotypes of planted propagules (Peterson et al. 2011, Raymond et al. 2013).

The extent and scale of the changes in ecological systems expected under climate change present a significant challenge to management. Changes in the size, severity, and frequency of disturbances will not be preventable, and further uncertainty arises from multiple-fire interactions (Teske et al. 2012, Larson et al. 2013, Parks et al. 2014), other disturbance agents such as bark beetles (Hicke et al. 2012), direct stress from climate on vegetation (Anderegg et al. 2013), and changes in biotic interactions (HilleRisLambers et al. 2013). The need to incorporate uncertainty and non-stationarity explicitly in monitoring, recognizing, and adapting to change will be heightened under future climate.

Conclusions

We draw three main conclusions from this study. First, variation in burn severity within a fire has a more direct influence on the postfire landscape pattern than does fire size alone. Therefore, it is essential to know if observed and predicted increases in area burned translate into changes in the severity and spatial pattern of severity. We found a positive relationship between fire size and burn severity, and between fire size and high-severity patch size and patch interior in the northern Cascade Range. Thus, our second conclusion is that if these statistical relationships persist under future climate, and subsequent successional processes and overlapping disturbances do not ameliorate the homogenizing influences of large high-severity fires, then the landscape pattern as a whole may shift to a more homogeneous state, impacting ecosystem functions at both local and large scales. Third, the impact of changing climate and weather on the spatial attributes of fire regimes will be mediated by the strength of local bottom-up controls. In each of the four subsections within the larger study area, the relationship between fire size and both severity and severity pattern differed, reflecting each subsection's vegetation, fuels, topography, and climate. Local controls may continue to be important in low- and mixed-severity fire regimes, even under climate conducive to large fires. In contrast, the change of controls from local bottom-up factors to top-down factors is likely to be most pronounced in high-severity fire regimes with already weak "bottom-up" local controls.

Acknowledgments

The authors thank the MTBS staff, particularly Stephen Howard of the EROS Data Center, Sioux Falls, for assistance in developing and processing the burn-severity data used in this project. Andrew Larson, Jim Lutz, Maureen Kennedy, Sandra Haire, Paul Hessburg, Susan Prichard, and an anonymous reviewer provided constructive and helpful reviews of the manuscript. Robert Norheim consulted on GIS analysis and produced Fig. 1. Funding for this research was provided by the U.S. Forest Service, Pacific Northwest Research Station, through a cooperative agreement with the University of Washington, School of Environmental and Forest Sciences.

Literature Cited

Abatzoglou, J., and C. Kolden. 2013. Relationships between climate and macroscale area burned in the western United States. International Journal of Wildland Fire 22:1003–1020.

Agee, J. K. 1993. Fire ecology of Pacific Northwest forests. Island Press. Washington, D.C., USA.

Agee, J. K. 1997. The severe weather wildfire—Too hot to handle? Northwest Science 71:153–156.

Agee, J. K., M. Finney, and R. de Gouvenain. 1990. Forest fire history of Desolation Peak, Washington. Canadian Journal of Forest Research 20:350–356.

Agee, J. K., et al. 1985. Vegetation and fuel mapping of North Cascades National Park Service Complex. Final report CX-9000-3-E029. National Park Service, Cooperative Park Studies Unit, College of Forest Resources, University of Washington, Seattle, Washington, USA.

Anderegg, W. R. L., J. M. Kane, and L. D. L. Anderegg. 2013. Consequences of widespread tree mortality triggered by drought and temperature stress. Nature Climate Change 3:30–36.

Bessie, W., and E. Johnson. 1995. The relative importance of fuels and weather on fire behavior in subalpine forests. Ecology 76:747–762.

Bowman, D. M., B. P. Murphy, M. M. Boer, R. A. Bradstock, G. J. Cary, M. A. Cochrane, R. J. Fensham, M. A. Krawchuk, O. F. Price, and R. J. Williams. 2013. Forest fire management, climate change, and the risk of catastrophic carbon losses. Frontiers in Ecology and the Environment 11:66–68.

Brubaker, L. 1986. Responses of tree populations to climatic change. Plant Ecology 67:119–130.

Buchalski, M. R., J. B. Fontaine, P. A. Heady III, J. P. Hayes, and W. F. Frick. 2013. Bat response to differing fire severity in mixed-conifer forest, California, USA. PLoS ONE 8:e57884.

Cansler, C. A. 2011. Drivers of burn severity in the northern Cascade Range, Washington, USA. Thesis. University of Washington, Seattle, Washington, USA. http://hdl.handle.net/1773/16539

Cansler, C. A., and D. McKenzie. 2012. How robust are burn severity indices when applied in a new region? Evaluation of alternate field-based and remote-sensing methods. Remote Sensing 4:456–483.

Churchill, D. J., A. J. Larson, M. C. Dahlgreen, J. F. Franklin, P. F. Hessburg, and J. A. Lutz. 2013. Restoring forest resilience: From reference spatial patterns to silvicultural prescriptions and monitoring. Forest Ecology and Management 291:442–457.

Cleland, D. T., P. E. Avers, W. H. McNab, M. E. Jensen, R. G. Bailey, T. King, and W. E. Russell. 1997. National hierarchical framework of ecological units. Pages 181–200 *in* M. S. Boyce and A. Harney, editors. Ecosystem management applications for sustainable forest and wildlife resources. Yale University Press, New Haven, Connecticut, USA.

Collins, B. M., J. D. Miller, A. E. Thode, M. Kelly, J. W. van Wagtendonk, and S. L. Stephens. 2009. Interactions among wildland fires in a long-established Sierra Nevada natural fire area. Ecosystems 12:114–128.

Collins, B. M., and S. L. Stephens. 2010. Stand-replacing patches within a "mixed severity" fire regime: quantitative characterization using recent fires in a long-established natural fire area. Landscape Ecology 25:927–939.

Cushman, S., K. McGarigal, and M. Neel. 2008. Parsimony in landscape metrics: Strength, universality, and consistency. Ecological Indicators 8:691–703.

Daly, C., W. P. Gibson, G. H. Taylor, G. L. Johnson, and P. Pasteris. 2002. A knowledge-based approach to the statistical mapping of climate. Climate Research 22:99–113.

Dillon, G. K., Z. A. Holden, P. Morgan, M. A. Crimmins, E. K. Heyerdahl, and C. H. Luce. 2011. Both topography and climate affected forest and woodland burn severity in two regions of the western US, 1984 to 2006. Ecosphere 2:art130.

Donato, D. C., J. B. Fontaine, J. L. Campbell, W. D. Robinson, J. B. Kauffman, and B. E. Law. 2009. Conifer regeneration in stand-replacement portions of a large mixed-severity wildfire in the Klamath–Siskiyou Mountains. Canadian Journal of Forest Research 39:823–838.

Dudley, J. G., V. A. Saab, and J. P. Hollenbeck. 2012. Foraging-habitat selection of Black-backed Woodpeckers in forest burns of southwestern Idaho. Condor 114:348–357.

Duffy, P. A., J. Epting, J. M. Graham, T. S. Rupp, and A. D. McGuire. 2007. Analysis of Alaskan burn severity patterns using remotely sensed data. International Journal of Wildland Fire 16:277–284.

ECOMAP. 2007. Delineation, peer review, and refinement of subregions of the conterminous United States. USDA General Technical Report WO-76A. USDA Forest Service, Washington, D.C., USA. http://fsgeodata.fs.fed.us/other_resources//ecosubregions.php

Eidenshink, J., B. Schwind, K. Brewer, Z. Zhu, B. Quayle, and S. Howard. 2007. A project for monitoring trends in burn severity. Fire Ecology 3:3–21.

Fahnestock, G. R. 1976. Fires, fuel, and flora as factors in wilderness management: the Pasayten case. Proceedings of the Tall Timbers Fire Ecology Conference 15:33–70.

Flannigan, M. D., A. S. Cantin, W. J. de Groot, M. Wotton, A. Newbery, and L. M. Gowman. 2013. Global wildland fire season severity in the 21st century. Forest Ecology and Management 294:54–61.

Flannigan, M. D., M. A. Krawchuk, W. J. de Groot, B. M. Wotton, and L. M. Gowman. 2009. Implications of changing climate for global wildland fire. International Journal of Wildland Fire 18:483–507.

Franklin, J. F., and C. T. Dyrness. 1988. Natural vegetation of Oregon and Washington. Second edition. Oregon State University Press, Corvallis, Oregon, USA.

Haire, S. L., and K. McGarigal. 2009. Changes in fire severity across gradients of climate, fire size, and topography: A landscape ecological perspective. Fire Ecology 5:86–103.

Haire, S. L., and K. McGarigal. 2010. Effects of landscape patterns of fire severity on regenerating ponderosa pine forests (*Pinus ponderosa*) in New Mexico and Arizona, USA. Landscape Ecology 25:1055–1069.

Haire, S. L., K. McGarigal, and C. Miller. 2013. Wilderness shapes contemporary fire size distributions across landscapes of the western United States. Ecosphere 4:1–20.

Hessburg, P. F., J. K. Agee, and J. F. Franklin. 2005. Dry forests and wildland fires of the inland Northwest USA: Contrasting the landscape ecology of the pre-settlement and modern eras. Forest Ecology and Management 211:117–139.

Hessburg, P. F., R. B. Salter, and K. M. James. 2007. Re-examining fire severity relations in pre-management era mixed conifer forests: inferences from landscape patterns of forest structure. Landscape Ecology 22:5–24.

Heyerdahl, E. K., D. McKenzie, L. D. Daniels, A. E. Hessl, J. S. Littell, and N. J. Mantua. 2008*a*. Climate drivers of regionally synchronous fires in the inland Northwest (1651–1900). International Journal of Wildland Fire 17:40–49.

Heyerdahl, E. K., P. Morgan, and J. P. Riser. 2008*b*. Multi-season climate synchronized historical fires in dry forests (1650–1900), northern Rockies, USA. Ecology 89:705–716.

Hicke, J. A., M. C. Johnson, J. L. Hayes, and H. K. Preisler. 2012. Effects of bark beetle-caused tree mortality on wildfire. Forest Ecology and Management 271:81–90.

HilleRisLambers, J., M. A. Harsch, A. K. Ettinger, K. R. Ford, and E. J. Theobald. 2013. How will biotic interactions influence climate change-induced range shifts? Annals of the New York Academy of Sciences 1297:112–125.

Holling, C. S. 1973. Resilience and stability of ecological systems. Annual Review of Ecology and Systematics 4:1–23.

Hunter, M. E., J. M. Iniguez, and L. B. Lentile. 2011. Short- and long-term effects on fuels, forest structure, and wildfire potential from prescribed fire and resource benefit fire in southwestern forests, USA. Fire Ecology 7:108–121.

Keane, R. E., J. K. Agee, P. Fulé, J. E. Keeley, C. Key, S. G. Kitchen, R. Miller, and L. A. Schulte. 2008. Ecological effects of large fires on US landscapes: benefit or catastrophe? International Journal of Wildland Fire 17:696–712.

Kennedy, M. C., and D. McKenzie. 2010. Using a stochastic model and cross-scale analysis to evaluate controls on historical low-severity fire regimes. Landscape Ecology 25:1561–1573.

Kutner, M. C., C. J. Nachtsheim, J. Neter, and W. Li. 2005. Applied linear statistical models. Fifth edition. McGraw-Hill, Boston, Massachusetts, USA.

Larson, A. J., R. T. Belote, C. A. Cansler, S. A. Parks, and M. S. Dietz. 2013. Latent resilience in ponderosa pine forest: effects of resumed frequent fire. Ecological Applications 23:1243–1249.

Larson, A. J., and D. Churchill. 2012. Tree spatial patterns in fire-frequent forests of western North America, including mechanisms of pattern formation and implications for designing fuel reduction and restoration treatments. Forest Ecology and Management 267:74–92.

Lentile, L. B., P. Morgan, A. T. Hudak, M. J. Bobbitt, S. A. Lewis, A. M. S. S. Smith, and P. R. Robichaud. 2007. Post-fire burn severity and vegetation response following eight large wildfires across the western United States. Fire Ecology 3:91–108.

Levin, S. A. 1992. The problem of pattern and scale in ecology: The Robert H. MacArthur Award lecture. Ecology 73:1943–1967.

Littell, J. S., D. McKenzie, D. L. Peterson, and A. L. Westerling. 2009. Climate and wildfire area burned in western U.S. ecoprovinces, 1916–2003. Ecological Applications 19:1003–1021.

Littell, J. S., E. E. Oneil, D. McKenzie, J. A. Hicke, J. A. Lutz, R. A. Norheim, and M. M. Elsner. 2010. Forest ecosystems, disturbance, and climatic change in Washington State, USA. Climatic Change 102:129–158.

Lorenz, T. J., K. A. Sullivan, A. V. Bakian, and C. A. Aubry. 2011. Cache-site selection in Clark's Nutcracker (*Nucifraga columbiana*). Auk 128:237–247.

Lutz, J. A., C. H. Key, C. A. Kolden, J. T. Kane, and J. W. van Wagtendonk. 2011. Fire frequency, area burned, and severity: A quantitative approach to defining a normal fire year. Fire Ecology 7:51–65.

Lutz, J. A., J. W. van Wagtendonk, A. E. Thode, J. D. Miller, and J. F. Franklin. 2009. Climate, lightning ignitions, and fire severity in Yosemite National Park, California, USA. International Journal of Wildland Fire 18:765–774.

Lydersen, J., and M. North. 2012. Topographic variation in structure of mixed-conifer forests under an active-fire regime. Ecosystems 15:1134–1146.

Lyons-Tinsley, C., and D. L. Peterson. 2012. Surface fuel treatments in young, regenerating stands affect wildfire severity in a mixed conifer forest, eastside Cascade Range, Washington, USA. Forest Ecology and Management 270:117–125.

McCaughey, W. W., W. C. Schmidt, and R. C. Shearer. 1986. Seed-dispersal characteristics of conifers in the inland mountain west. Pages 50–62 *in* R. C. Shearer, compiler. Proceedings—Conifer Tree Seed in the Inland Mountain West Symposium. General Technical Report INT-GRT-203. USDA Forest Service, Intermountain Research Station, Ogden, Utah, USA.

McGarigal, K., S. A. Cushman, M. C. Neel, and E. Ene. 2002. FRAGSTATS: Spatial pattern analysis program for categorical maps. Version 3.3. University of Massachusetts, Amherst, Massachusetts, USA. http://www.umass.edu/landeco/research/fragstats/fragstats.html

McKenzie, D., Z. Gedalof, D. L. Peterson, and P. Mote. 2004. Climatic change, wildfire, and conservation. Conservation Biology 18:890–902.

McKenzie, D., and M. C. Kennedy. 2011. Scaling laws and complexity in fire regimes. Chapter 2 *in* D. McKenzie, C. Miller, and D. A. Falk, editors. 2011. The landscape ecology of fire. Springer, Dordrecht, The Netherlands.

McKenzie, D., and M. C. Kennedy. 2012. Power laws reveal phase transitions in landscape controls of fire regimes. Nature Communications 3:726–730.

McKenzie, D., and J. S. Littell. 2011. Climate change and wilderness fire regimes. International Journal of Wilderness 17:22–27.31.

McKenzie, D., C. Miller, and D. A. Falk. 2011. Synthesis: landscape ecology and changing fire regimes. Pages 295–303 *in* D. McKenzie, C. Miller, and D. A. Falk, editors. The landscape ecology of fire. Springer, Dordrecht, The Netherlands.

Meigs, G. W., D. C. Donato, J. L. Campbell, J. G. Martin, and B. E. Law. 2009. Forest fire impacts on carbon uptake, storage, and emission: The role of burn severity in the Eastern Cascades, Oregon. Ecosystems 12:1246–1267.

Miller, J. D., B. M. Collins, J. A. Lutz, S. L. Stephens, J. W. van Wagtendonk, and D. A. Yasuda. 2012*b*. Differences in wildfires among ecoregions and land management agencies in the Sierra Nevada region, California, USA. Ecosphere 3:1–20.

Miller, J. D., E. E. Knapp, C. H. Key, C. N. Skinner, C. J. Isbell, R. M. Creasy, and J. W. Sherlock. 2009*a*. Calibration and validation of the Relative differenced Normalized Burn Ratio (RdNBR) to three measures of fire severity in the Sierra Nevada and Klamath Mountains, California, USA. Remote Sensing of Environment 113:645–656.

Miller, J. D., H. D. Safford, M. Crimmins, and A. E. Thode. 2009*b*. Quantitative evidence for increasing forest fire severity in the Sierra Nevada and southern Cascade Mountains, California and Nevada, USA. Ecosystems 12:16–32.

Miller, J. D., C. N. Skinner, H. D. Safford, E. E. Knapp, and C. M. Ramirez. 2012*a*. Trends and causes of severity, size, and number of fires in northwestern California, USA. Ecological Applications 22:184–203.

Miller, J. D., and A. E. Thode. 2007. Quantifying burn severity in a heterogeneous landscape with a relative version of the delta Normalized Burn Ratio (dNBR). Remote Sensing of Environment 109:66–80.

Moritz, M. A., P. F. Hessburg, and N. A. Povak. 2011. Native fire regimes and landscape resilience. Pages 51–86 *in* D. McKenzie, C. Miller, and D. A. Falk, editors. The landscape ecology of fire. Springer, Dordrecht, The Netherlands.

Mote, P. W., and E. P. Salathé. 2010. Future climate in the Pacific Northwest. Climatic Change 102:29–50.

Neary, D. G., C. C. Klopatek, L. F. DeBano, and P. F. Ffolliott. 1999. Fire effects on belowground sustainability: a review and synthesis. Forest Ecology and Management 122:57–71.

Neel, M. C., K. McGarigal, and S. A. Cushman. 2004. Behavior of class-level landscape metrics across gradients of class aggregation and area. Landscape Ecology 19:435–455.

North, M., B. M. Collins, and S. Stephens. 2012. Using fire to increase the scale, benefits, and future maintenance of fuels treatments. Journal of Forestry 110:392–401.

Parks, S. A., C. Miller, C. R. Nelson, and Z. A. Holden. 2014. Previous fires moderate burn severity of subsequent wildland fires in two large western US wilderness areas. Ecosystems 17:29–42.

Perry, D. A., P. F. Hessburg, C. N. Skinner, T. A. Spies, S. L. Stephens, A. H. Taylor, J. F. Franklin, B. McComb, and G. Riegel. 2011. The ecology of mixed severity fire regimes in Washington, Oregon, and Northern California. Forest Ecology and Management 262:703–717.

Peterson, D. L., C. I. Millar, L. A. Joyce, M. J. Furniss, J. E. Halofsky, R. P. Neilson, and T. L. Morelli. 2011. Responding to climate change in national forests: A guidebook for developing adaptation options. USDA General Technical Report PNW-GTR-855, USDA Forest Service, Pacific Northwest Research Station, Portland, Oregon, USA.

Peterson, G. D. 2002. Contagious disturbance, ecological memory, and the emergence of landscape pattern. Ecosystems 5:329–338.

Pickett, S. T. A., and P. S. White. 1985. The ecology of natural disturbance and patch dynamics. Academic Press, New York, New York, USA.

Prichard, S. J., Z. Gedalof, W. W. Oswald, and D. L. Peterson. 2009. Holocene fire and vegetation dynamics in a montane forest, North Cascade Range, Washington, USA. Quaternary Research 72:57–67.

Prichard, S. J., and M. C. Kennedy. 2012. Fuel treatment effects on tree mortality following wildfire in dry mixed conifer forests, Washington State, USA. International Journal of Wildland Fire 21:1004–1013.

R Development Core Team. 2010. R: A language and environment for statistical computing. R Foundation for Statistical Computing, Vienna, Austria. http://www.R-project.org/

Raymond, C. L., and D. McKenzie. 2012. Carbon dynamics of forests in Washington, USA: 21st century projections based on climate-driven changes in fire regimes. Ecological Applications 22:1589–1611.

Raymond, C., D. Peterson, and R. Rochefort. 2013. The North Cascadia Adaptation Partnership: A science–management collaboration for responding to climate change. Sustainability 5:136–159.

Roberts, S. L., J. W. van Wagtendonk, A. K. Miles, D. A. Kelt, and J. A. Lutz. 2008. Modeling the effects of fire severity and spatial complexity on small mammals in Yosemite National Park, California. Fire Ecology 4:83–104.

Rollins, M. G., and C. K. Frame. 2006. The LANDFIRE Prototype Project: Nationally consistent and locally relevant geospatial data for wildland fire management. USDA General Technical Report RMRS-GTR-175. USDA Forest Service, Rocky Mountain Research Station, Fort Collins, Colorado, USA.

Savage, M., and J. Mast. 2005. How resilient are southwestern ponderosa pine forests after crown fires? Canadian Journal of Forest Research 35:967–977.

Savage, M., J. N. Mast, and J. J. Feddema. 2013. Double whammy: high-severity fire and drought in ponderosa pine forests of the Southwest. Canadian Journal of Forest Research 43:570–583.

Smithwick, E. A. H. 2011. Pyrogeography and biogeochemical resilience. Pages 143–164 *in* D. McKenzie, C. Miller, and D. A. Falk, editors. The landscape ecology of fire. Springer, Dordrecht, The Netherlands.

Soverel, N. O., D. D. B. Perrakis, and N. C. Coops. 2010. Estimating burn severity from Landsat dNBR and RdNBR indices across western Canada. Remote Sensing of Environment 114:1896–1909.

Sugihara, N. G., J. W. van Wagtendonk, and J. Fites-Kaufmann. 2006. Fire as an ecological process. Pages 58–74 *in* N. G. Sugihara, J. W. van Wagtendonk, K. E. Shaffer, J. Fites-Kaufman, and A. E. Thode, editors. Fire in California's ecosystems. University of California Press, Berkeley, California, USA.

Swanson, F. J. 1981. Fire and geomorphic processes. Pages 401–444 *in* H. A. Mooney, T. M. Bonnicksen, N. L. Christensen, J. E. Lotan, and W. A. Reiners, editors. Proceedings of the Conference on Fire Regimes and Ecosystem Properties. USDA Forest Service General Technical Report WO-26, USDA, Washington, D.C., USA.

Swanson, M. E., J. F. Franklin, R. L. Beschta, C. M. Crisafulli, D. A. DellaSala, R. L. Hutto, D. B. Lindenmayer, and F. J. Swanson. 2011. The forgotten stage of forest succession: early-successional ecosystems on forest sites. Frontiers in Ecology and the Environment 9:117–125.

Taleb, N. N. 2012. Anti-fragile: Things that gain from disorder. Random House, New York, New York, USA.

Teske, C. C. 2012. Fire-on-fire interactions in three large wilderness areas. Dissertation. University of Idaho, Moscow, Idaho, USA.

Teske, C. C., C. A. Seielstad, and L. P. Queen. 2012. Characterizing fire-on-fire interactions in three large wilderness areas. Fire Ecology 8:82–106.

Thompson, J. R., and T. A. Spies. 2009. Vegetation and weather explain variation in crown damage within a large mixed-severity wildfire. Forest Ecology and Management 258:1684–1694.

Turner, M. G., W. W. Hargrove, R. H. Gardner, and W. H. Romme. 1994. Effects of fire on landscape heterogeneity in Yellowstone National Park, Wyoming. Journal of Vegetation Science 5:731–742.

Turner, M. G., and W. H. Romme. 1994. Landscape dynamics in crown fire ecosystems. Landscape Ecology 9:59–77.

Turner, M. G., W. H. Romme, and R. H. Gardner. 1999. Prefire heterogeneity, fire severity, and early postfire plant reestablishment in subalpine forests of Yellowstone National Park, Wyoming. International Journal of Wildland Fire 9:21–36.

Turner, M. G., W. H. Romme, R. H. Gardner, and W. W. Hargrove. 1997. Effects of fire size and pattern on early succession in Yellowstone National Park. Ecological Monographs 67:411–433.

van Nes, E. H., and M. Scheffer. 2005. Implications of spatial heterogeneity for catastrophic regime shifts in ecosystems. Ecology 86:1797–1807.

van Wagtendonk, J. W., and J. A. Lutz. 2007. Fire regime attributes of wildland fires in Yosemite National Park, USA. Fire Ecology 3:34–52.

Vander Wall, S. B. 2008. On the relative contributions of wind vs. animals to seed dispersal of four Sierra Nevada pines. Ecology 89:1837–1849.

Westerling, A. L., M. G. Turner, E. A. H. Smithwick, W. H. Romme, and M. G. Ryan. 2011. Continued warming could transform Greater Yellowstone fire regimes by mid-21st century. Proceedings of the National Academy of Sciences USA 108:13165–13170.

Whittaker, R. 1960. Vegetation of the Siskiyou Mountains, Oregon and California. Ecological Monographs 30:279–338.

Wightman, C. S., V. A. Saab, C. Forristal, K. Mellen-McLean, and A. Markus. 2010. White-headed woodpecker nesting ecology after wildfire. Journal of Wildlife Management 74:1098–1106.

Wotton, B. M., C. A. Nock, and M. D. Flannigan. 2010. Forest fire occurrence and climate change in Canada. International Journal of Wildland Fire 19:253–271.

Supplemental Material

Appendix A

Tables and figures showing supplemental methods including (1) study area maps, (2) topographical complexity metrics, (3) burn severity class descriptions, (4) spatial pattern metric equations, and (5) fires included in the study (*Ecological Archives* A024-060-A1).

Appendix B

Tables and figures showing supplemental results including (1) climate regression models, (2) subsection-scale severity pattern statistics and patch distributions, and (3) a sensitivity analysis of the effect of core area distances on regression model results (*Ecological Archives* A024-060-A2).